

**Numerical investigation of flow around two co-rotating cylinders in
side by side configuration**



By

Moaqir Ahmad Mian

(Registration No: 00000328915)

Department of Mechanical Engineering

School of Mechanical and Manufacturing Engineering

National University of Sciences & Technology (NUST)

Islamabad, Pakistan

(2024)

Numerical investigation of flow around two co-rotating cylinders in side by side configuration



By

Moaqir Ahmad Mian

(Registration No: 00000328915)

A thesis submitted to the National University of Sciences and Technology, Islamabad,

in partial fulfillment of the requirements for the degree of

Master of Science in
Mechanical Engineering

Supervisor: Dr. Muhammad Nafees Mumtaz Qadri

Co-Supervisor: Dr. Adnan Munir

School of Mechanical and Manufacturing Engineering

National University of Sciences & Technology (NUST)

Islamabad, Pakistan

(2024)

THESIS ACCEPTANCE CERTIFICATE

Certified that final copy of MS Thesis written by Mr Moaqir Ahmad Mian (Registration No. 328915, of School Of Mechanical And Manufacturing Engineering has been vetted by undersigned, found complete in all respects as per NUST Statutes/ Regulations/ Masters Policy, is free of plagiarism, errors, and mistakes and is accepted as partial fulfillment for award of Masters degree. It is further certified that necessary amendments as point out by GEC members and foreign/ local evaluators of the scholar have also been incorporated in the said thesis.

Signature:

A handwritten signature in blue ink, appearing to read 'M Nafees Mumtaz Qadri', with a horizontal line underneath.

Name of Supervisor Dr M Nafees Mumtaz Qadri

Date: 13th August 2024

Signature (HOD):

A handwritten signature in blue ink, appearing to read 'Emad', with a horizontal line underneath.

Date: 13th August 2024

Signature (Dean/ Principal)

A handwritten signature in blue ink, appearing to read 'J. Qadri', with a horizontal line underneath.

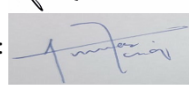
Date: 13th August 2024



National University of Sciences & Technology (NUST)
MASTER'S THESIS WORK

We hereby recommend that the dissertation prepared under our supervision by: Moaqir ahmad Mian (00000328915)
Titled: Numerical investigation of flow around two co-rotating cylinders in side by side configuration be accepted in partial fulfillment of the requirements for the award of MS in Mechanical Engineering degree.

Examination Committee Members

- | | | |
|----|-------------------|--|
| 1. | Name: Adnan Munir | Signature:  |
| 2. | Name: Emad Ud Din | Signature:  |
| 3. | Name: Zaib Ali | Signature:  |
| 4. | Name: Ammar Tariq | Signature:  |

Supervisor: Muhammad Nafees Mumtaz Qadri

Signature: 

Date: 13 - Aug - 2024



Head of Department

13 - Aug - 2024

Date

COUNTERSIGNED

13 - Aug - 2024

Date



Dean/Principal

CERTIFICATE OF APPROVAL

This is to certify that the research work presented in this thesis, entitled “**Numerical investigation of flow around two co-rotating cylinders in side by side configuration**” was conducted by Mr. **Moaqir Ahmad Mian** under the supervision of **Dr Muhammad Nafees Mumtaz Qadri**.

No part of this thesis has been submitted anywhere else for any other degree. This thesis is submitted to the **Department of Mechanical Engineering** in partial fulfillment of the requirements for the degree of Master of Science in Field of Mechanical Engineering.

Department of Mechanical Engineering National University of Sciences and Technology, Islamabad.

Student Name: Moaqir Ahmad Mian

Signature:

Examination Committee:

a) Dr Adnan Munir (Co-Supervisor)

Signature:

Assistant Professor, ME Dept, SMME, NUST

b) Dr Emad-ud-din

Signature:

Professor, ME Dept, SMME, NUST

c) Dr Zaib Ali

Signature:

Associate Professor, ME Dept, SMME, NUST

d) Dr Ammar Tariq

Signature:

Assistant Professor, ME Dept, SMME, NUST

Supervisor Name: Dr Muhammad Nafees Mumtaz Qadri

Signature:

Name of Dean/HOD: Dr Mian Ashfaq Ali

Signature:

AUTHOR'S DECLARATION

I Moqir Ahmad Mian hereby state that my MS thesis titled “Numerical Investigation Of Flow Around Two Co-Rotating Cylinders In Side By Side Configuration” is my own work and has not been submitted previously by me for taking any degree from National University of Sciences and Technology, Islamabad or anywhere else in the country/ world.

At any time if my statement is found to be incorrect even after I graduate, the university has the right to withdraw my MS degree.

Name of Student: Moqir Ahmad Mian

Date: 19-8-2024

PLAGIARISM UNDERTAKING

I solemnly declare that research work presented in the thesis titled “**Numerical investigation of flow around two co-rotating cylinders in side by side configuration**” is solely my research work with no significant contribution from any other person. Small contribution/ help wherever taken has been duly acknowledged and that complete thesis has been written by me.

I understand the zero tolerance policy of the HEC and National University of Sciences and Technology (NUST), Islamabad towards plagiarism. Therefore, I as an author of the above titled thesis declare that no portion of my thesis has been plagiarized and any material used as reference is properly referred/cited.

I undertake that if I am found guilty of any formal plagiarism in the above titled thesis even after award of MS degree, the University reserves the rights to withdraw/revoke my MS degree and that HEC and NUST, Islamabad has the right to publish my name on the HEC/University website on which names of students are placed who submitted plagiarized thesis.

Student Signa 

Name: Moaqir Ahmad Mian

DEDICATION

This is dedicated to my exceptional parents, wife, son , adored siblings, and friends, whose tremendous support and cooperation led me to this outstanding accomplishment.

ACKNOWLEDGEMENTS

I am thankful to my Creator, Allah Subhana-Watala, for guiding me through this work at every step and for every new thought You set in my mind to improve it. Indeed, I could have done nothing without your priceless help and guidance. Whosoever helped me throughout my thesis, whether my parents or any other individual, was Your will, so indeed, none is worthy of praise but You.

I am profusely thankful to my beloved parents, who raised me when I could not walk and continued to support me throughout every aspect of my life.

I would also like to express special thanks to my supervisor, Dr. Muhammad Nafees Mumtaz Qadri, for his help throughout my thesis, for CFD, and for providing computational resources.

We would also like to thank Bilal Ali for his tremendous support and cooperation. Each time I got stuck in something; he came up with a solution. Without his help, I wouldn't have been able to complete my thesis. I appreciate his patience and guidance throughout the whole dissertation.

I would also like to thank my co-supervisors for being on my thesis guidance and evaluation committee and express my special thanks to Dr. Adnan Munir for his help. I am also thankful to Muhammad Ibrahim and Yashfa Ashraf for their support and cooperation.

Finally, I would like to express my gratitude to all the individuals who have helped me with my studies.

TABLE OF CONTENTS

ACKNOWLEDGEMENTS	VIII
TABLE OF CONTENTS	IX
LIST OF FIGURES	XI
LIST OF SYMBOLS, ABBREVIATIONS AND ACRONYMS	XIII
ABSTRACT	XIV
CHAPTER 1: INTRODUCTION	1
1.1 Introduction	1
1.2 Literature review	1
1.2.1 Flow Around Rotating Cylinders	5
1.2.2 Vortex Shedding and Drag Reduction	6
1.2.3 Heat Transfer in Rotating Cylinders	6
1.2.4 Effects of Cylinder Arrangement	7
1.2.5 Fluid Dynamics and Numerical Simulations	7
1.2.6 Experimental and Computational Studies	7
1.2.7 Low Reynolds Number Flow Characteristics for Two Side by Side Rotating Circular Cylinders	8
1.2.8 Control of Vortex Shedding from Two Side-by-Side Cylinders	9
1.2.9 Effect of Rotational Speed on the Stability of Two Rotating Side-by-Side Circular Cylinders at Low Reynolds Number	10
1.2.10 Numerical Investigation of Flow Across Three Co-Rotating Cylinders	11
1.2.12 Vortex-Induced Vibrations of Two Mechanically Coupled Circular Cylinders	14
1.2.13 Flow Interference for VIV Responses of Adjacent Cylinders	15
CHAPTER 2: NUMERICAL MODELING	17
2.1 Introduction	17
2.2 Navier Stokes Equations	17
2.2.1 Introduction	17
2.2.2 Derivation of the 2-D Navier-Stokes Equations	17
2.3 Computational Domain and Boundary Conditions	20
2.4 Mesh Independence Study	21
2.5 Numerical Method	24
2.6 Validation Case	25
CHAPTER 3: RESULTS AND DISCUSSION	27
3.1 Introduction	27
3.2 Flow Structures	27
3.3 Wake Structures	27
3.4 Effect of Cylinder Spacing	28

3.5	Effect of Rotational Speed	28
3.5	Discussion	29
3.5.1	Gap Ratio of 0.5 ($g^* = 0.5$)	29
3.5.2	Gap spacing of 1 ($g^* = 1$)	36
3.5.3	Gap Ratio of 3.0 ($g^* = 3.0$)	40
3.5.4	Dynamic Mode Decomposition	45
CHAPTER4: CONCLUSION AND FUTURE RECOMMENDATIONS		48
REFERENCES		51

LIST OF FIGURES

	Page No.
Figure 1-1 (Color online available at journals.cambridge.org/FLM) Idealized synchronized vortex shedding modes in the wake of a non-rotating cylinder pair. Flow is from left to right. (a) In-phase shedding. (b) Anti-phase shedding.	2
Figure 1-2 Counter-rotating circular cylinder pair. (a) Doublet-like configuration. (b) Reverse doublet-like configuration.....	3
Figure 2-1 Methodology	22
Figure 2-2 Computational domain for the flow	23
Figure 2-3 Structured Mesh used in this study	23
Figure 2-4 Optimal mesh close up view	24
Figure 2-5 Mesh Independence Study	24
Figure 2-6 Validation Case	25
Figure 3-1 <i>Time histories</i> $\alpha = 3.0$ $g^* = 0.5$ $Re = 50$	31
Figure 3-2 <i>Time histories</i> $\alpha = 3.0$ $g^* = 0.5$ $Re = 100$	31
Figure 3-3 vorticity plot at $\alpha = 3.0$ $g^* = 0.5$ $Re = 50$	33
Figure 3-4 Vorticity plot at $\alpha = 3.0$ $g^* = 0.5$ $Re = 100$	33
Figure 3-5 <i>Time histories</i> $\alpha = 3.5$ $g^* = 0.5$ $Re = 50$	33
Figure 3-6 vorticity plots at $\alpha = 3.5$ $g^* = 0.5$ $Re = 50$	33
Figure 3-7 <i>Time histories</i> $\alpha = 3.5$ $g^* = 0.5$ $Re = 100$	34
Figure 3-8 vorticity Plot at $\alpha = 3.5$ $g^* = 0.5$ $Re = 100$	34
Figure 3-9 <i>Time histories</i> $\alpha = 4.0$ $g^* = 0.5$ $Re = 50$	34
Figure 3-10 vorticity plot at $\alpha = 4.0$ $g^* = 0.5$ $Re = 50$	34
Figure 3-11 <i>Time histories</i> $\alpha = 4.0$ $g^* = 0.5$ $Re = 100$	35
Figure 3-12 Vorticity plots at $\alpha = 4.0$ $g^* = 0.5$ $Re = 100$	35
Figure 3-13 <i>Mean Cl</i> $g^* = 0.5$ $Re = 50$	35
Figure 3-14 <i>Mean Cl</i> $g^* = 0.5$ $Re = 100$	35
Figure 3-15 $\alpha = 1.5$ $g^* = 0.5$ <i>Stable</i> at $Re = 50$	35
Figure 3-16 $\alpha = 1.5$ $g^* = 0.5$ <i>Unstable</i> at $Re = 100$	35
Figure 3-17 <i>Mean drag</i> $g^* = 0.5$ $Re = 50$	36
Figure 3-18 <i>Mean drag</i> $g^* = 0.5$ $Re = 100$ (right)	36
Figure 3-19 Virtual Body at $\alpha = 4.0$ $g^* = 0.5$ $Re = 50$	Error! Bookmark not defined.
Figure 3-20 <i>Time histories</i> $\alpha = 3.0$ $g^* = 1$ <i>stable</i> at $Re = 50$	37
Figure 3-21 Vorticity plots at $\alpha = 3.0$ $g^* = 1$ $Re = 50$	37
Figure 3-23 <i>Time histories</i> $\alpha = 3.0$ $g^* = 1$ <i>unstable</i> at $Re = 100$ (right).....	37
Figure 3-24 vorticity plot at $\alpha = 3.0$ $g^* = 1$ $Re = 100$ <i>Unstable</i>	37
Figure 3-25 <i>Time histories</i> $\alpha = 3.5$ $g^* = 1$ <i>stable</i> at $Re = 50$	38
Figure 3-26 Vorticity plots at $\alpha = 3.5$ $g^* = 1$ $Re = 50$	38
Figure 3-27 <i>Time histories</i> $\alpha = 3.5$ $g^* = 1$ <i>stable</i> at $Re = 100$	38
Figure 3-28 Vorticity plots at $\alpha = 3.5$ $g^* = 1$ <i>stable</i> at $Re = 100$	38
Figure 3-29 <i>Time histories</i> $\alpha = 4.0$ $g^* = 1$ $Re = 50$	38
Figure 3-30 Vorticity plots at $\alpha = 4.0$ $g^* = 1$ <i>stable</i> at $Re = 50$	39

Figure 3-31 Time histories $\alpha = 4.0$ $g^* = 1$) $Re = 100$	39
Figure 3-32 Vorticity plots at $\alpha = 4.0$ $g^* = 1$ stable at $Re = 100$	39
Figure 3-33 Mean Cd $g^* = 1$ $Re = 50$	39
Figure 3-34 Mean Cd $g^* = 1$ $Re = 100$	39
Figure 3-35 Mean Cl $g^* = 1.0$ $Re = 50$	40
Figure 3-36 Mean Cl $g^* = 1.0$ $Re = 100$	40
Figure 3-37 Vortex wrapping at $\alpha = 3.5$ $g^* = 1$ stable at $Re = 100$. Error! Bookmark not defined.	
Figure 3-38 Time histories $\alpha = 1.5$ $g^* = 3$ stable at $Re = 50$	42
Figure 3-39 Vorticity plots at $\alpha = 1.5$ $g^* = 3$ stable at $Re = 50$ e	42
Figure 3-40 Time histories $\alpha = 1.5$ $g^* = 3$ unstable at $Re = 100$	42
Figure 3-41 Vorticity plots at $\alpha = 1.5$ $g^* = 3$ $Re = 100$	42
Figure 3-42 Time histories $\alpha = 2.0$ $g^* = 3$ stable at $Re = 50$	43
Figure 3-43 Vorticity plot at $\alpha = 2.0$ $g^* = 3$ at $Re = 50$	43
Figure 3-44 Time histories $\alpha = 2.0$ $g^* = 3$ unstable at $Re = 100$	43
Figure 3-45 Vorticity plot at $\alpha = 2$ $g^* = 3$ at $Re = 100$	43
Figure 3-46 Time histories $\alpha = 2.5$ $g^* = 3$ stable at $Re = 50$	44
Figure 3-47 $\alpha = 2.5$ $g^* = 3$ $Re = 50$	44
Figure 3-48 Time histories $\alpha = 2.5$ $g^* = 3$ at $Re = 100$	44
Figure 3-49 Vorticity plot at $\alpha = 2.5$ $g^* = 3$ stable at $Re = 100$	44
Figure 3-50 Time histories $\alpha = 4.0$ $g^* = 3$ stable at $Re = 50$	44
Figure 3-51 Time histories $\alpha = 4.0$ $g^* = 3$ at $Re = 100$	45
Figure 3-52 Secondary instability at $\alpha = 4.0$ $g^* = 3$ at $Re = 100$	45

LIST OF SYMBOLS, ABBREVIATIONS AND ACRONYMS

C_d	Drag Coefficient
C_l	Lift coefficient
α/ω	Non-dimensional rotational speed
Re	Reynolds number
$ D $	Diameter
g	Gap spacing
g^*	Non-dimensional gap spacing
t	time
T	Non dimensional time
U_∞	Free stream velocity
ρ	Density
VIV	vortex-induced vibration

ABSTRACT

This thesis investigates the fluid dynamics of co-rotating side-by-side cylinders under varying gap ratios (g^*) and Reynolds numbers (Re) to understand vortex suppression, drag reduction, and lift coefficient behaviors. Numerical simulations conducted with gap ratios of 0.5, 1, and 3 at $Re = 50$ and 100 reveal that increasing the gap spacing reduces vortex interaction, requiring higher critical rotational speeds for wake instability suppression. Despite this, low rotational speeds ($\alpha_{crit} > 3.5$) effectively stabilized the wake. At $Re = 50$, stable anti-phase drag coefficients and in-phase lift forces were observed below $\alpha_{crit} = 3.5$, with negative drag coefficients indicating thrust production. At $Re = 100$, the vortex street stabilized at $\alpha_{crit} = 3.5$ without secondary instability up to $\alpha = 5$. The study also identified the formation of small eddies and a virtual body at critical rotational speeds, impacting fluid dynamics and vortex suppression. These findings highlight the potential for optimizing rotational speeds and gap ratios to enhance fluid machinery performance, reduce energy consumption, and improve aerodynamic efficiency in aerospace, automotive, and marine engineering. This research extends previous studies, offering new strategies for fluid flow management and contributing valuable insights to the field of fluid dynamics.

Keywords: Vortex Suppression, Drag Reduction, Co-Rotating Cylinders, Wake Instability, vortex dynamics.

INTRODUCTION

1.1 Introduction

The vortex suppression and drag reduction of numerous cylinders in various configurations have been extensively investigated to enhance efficiency in different technical applications. In recent years, computer studies have been conducted on multiple side-by-side configurations to explore the relationship between the location of the cylinders and the reduction of drag. These studies aim to optimize the performance of the cylinders. In order to investigate the effect of the separation between two adjacent cylinders that rotate in the same direction of the suppression of vortices and the descent of drag in the system. The results of the current study are expected to provide valuable insights that will help in understanding the behavior of the system in general as well as how to design the system's technicality to have a more powerful and better performance.

1.2 Literature review

The interaction of the wakes of two non-rotating circular cylinders of equal diameter is determined by the Reynolds number and the non-dimensional gap spacing. The Reynolds number is a non-dimensional number that expresses the dependence of free stream flow rate and cylinder diameter on kinematic viscosity: The non-dimensional gap spacing was determined by the following ratio:

Previously, the work of Williamson and Xu, Zhou & So on unstable two-dimensional vortex wakes in the Reynolds number range from 100 to 200 revealed interesting data on the views of vortex shedding that can occur in this interval. It has been experimentally established that when the distance between two cylinders is less than 1, then the wake is spewed in an insensitive direction, and they can be divided into drop-out and von Karm' a vortex street types, depending on the distance. Kim & Durbin and Sumner et al. reframe this conclusion.

The wake will be shed in a coordinated manner when gap widths are between 1 and 5. In general, the mode is either in-phase or anti-phase. Williamson described the anti-phase

cases; a new characteristic of this mode is the “stability,” with each vortex’s shape preserved. The in-phase mode, by contrast, demonstrates instability and has a high likelihood resulting in non-sinusoidal fluctuations in lift and drag. In this matter, the mode becomes unstable when vortices of the opposite sign combine to form larger vortex cells. During the shedding mode initialization, a tripping approach may be used first to start the time marching routine; the “flow handles are synchronized.” Alternatively, a larger time step and a flow component not aligned with the wind may be added.

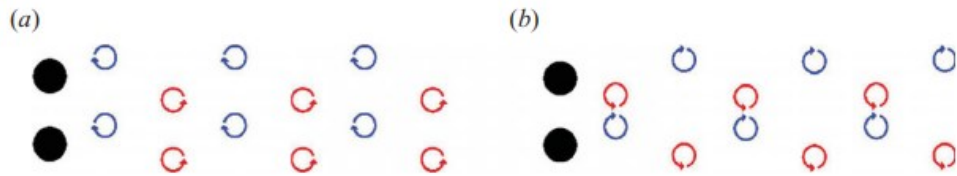


Figure 0-1 (Color online available at journals.cambridge.org/FLM) Idealized synchronized vortex shedding modes in the wake of a non-rotating cylinder pair. Flow is from left to right. (a) In-phase shedding. (b) Anti-phase shedding.

In recent years, several studies have demonstrated that counter-rotating two cylinders can minimize or even eliminate the instabilities present in their wake (Yoon et al. [5]; Chan & Jameson [6]). These two distinct rotational configurations, namely the doublet-like and reverse doublet-like, are shown in Figure 2. Yoon et al. [5] researched the doublet-like configuration for various gap distances at a Reynolds number of 100 and 50. Here, $\alpha = \omega/(2U/d)$, where ω is the rotational speed of the cylinders. Counter-rotating cylinders present a fascinating wake structure that can be classified according to the gap spacing between the cylinders and their rotational speed or angular velocity (α). For example, when the cylinders are rotated at speeds below the critical value, the wake structure depends on the gap (g^*) and the angular velocity. Chan and Jameson [6] found that, at a Reynolds number of 150 and a gap of 1, the critical angular velocity for their reverse doublet-like configuration was 1.5, which was lower than the necessary speed for the doublet-like configuration of 3.5 discovered a critical rotational speed, α_{crit} , which

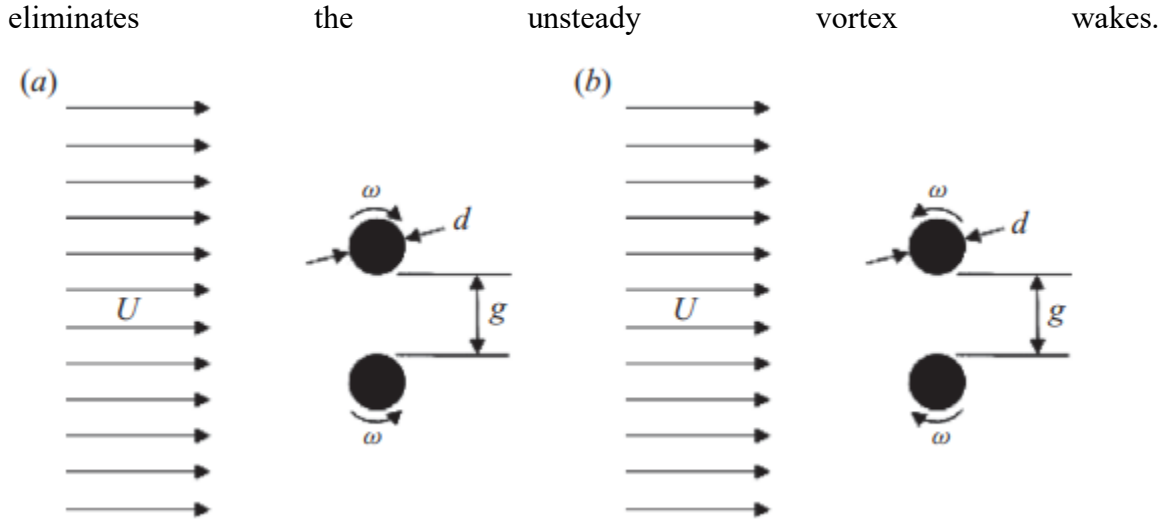


Figure 0-2 Counter-rotating circular cylinder pair. (a) Doublet-like configuration. (b) Reverse doublet-like configuration.

Building on this research, Andre S. Chan & Peter A. Dewey [7] have conducted additional investigations into the flow past two counter-rotating cylinders at the same rate. To explore the unsteady vortex wake, they utilized a high-order spectral difference method for compressible flow simulations and carried out experiments on a water channel. This paper has verified that the reduction in the space distance results in making the critical suppression rate diminish, resulting in synchronous or asynchronous VORTEX shedding, depending on the space. In the last decade, extensive research has been conducted on the behavior of rotating cylinder. The integration of the rotation cylinder by Shaafi et al. included a laminar boundary layer formed on a flat wall and one clocked and other counts difference rotating cylinder for using the number $Re = 100$. A non-dimensional space difference d^* between the cylinder and the flat wall of 0.1-3, and it was... The relationship that was studied currently provides new knowledge on the control of wake air flow, surface temperature, and heat flux during invariability within the Cylinder of pre-constant Re number. Rana et al. examined the vortex suppression regime in the gust response of a rotating cylinder between $d^* = 2$ and $d^* = 5$; $Re = 140$: they studied the lift and drag coefficients, the temperature field, and the Nusselt number. Bayat and Rahimi studied a rotating vertical cylinder flow; with $Re = 1, 5, 10, 15, 20 - Pr = 0.7$

They could predict the location of the cylinder stagnation point as a function of the Grashof and Richardson numbers. Thakur et al. [11] explored the flow around a rotating cylinder embedded in a channel filled with a power-law fluid at a range of Re numbers between 0.001 and 40. They found that, at a constant Re number, the wake length increases with the increasing degree of shear-thinning behavior and symmetry, and the flow transitions to an unsteady regime. These studies have provided valuable insight into the flow around rotating cylinders.

Placing a smaller circular cylinder can regulate fluid forces on a large circular cylinder near it. This methodology has been explored by Strykowski and Sreenivasan [12], who studied the effects of vortex shedding on a circular cylinder at low Reynolds Numbers. Subsequently, Sakamoto et al. [13] and Sakamoto and Haniu [14] examined the suppression of the fluid forces acting on square and circular cylinders at high Reynolds Numbers in a subcritical regime. Dalton et al. [15] also conducted numerical simulations to analyse the lift force suppression caused by a small circular cylinder on a large one.

Researchers have classified the techniques for suppressing fluid forces into two categories: one that relies on the control of the boundary layer and the other based on the control of the shear layers detached from the cylinder surface. These methods have successfully reduced the fluid forces acting on large circular cylinders and continue to be researched today.

Flow characteristics are highly dependent on the gap width between two cylinders. Despite this, research has focused chiefly on flow pattern changes in varying gap widths and the physical effects of these changes without much consideration for the influence of the Reynolds number. To better understand the impact of Reynolds number, Williamson [1] conducted experiments with relatively low Reynolds numbers ranging from 40 to 160 and found that synchronized vortex shedding could occur in both in-phase and antiphase forms, forming distinct vortex streets. Furthermore, Akinaga and Mizushima [16] used linear stability theory to calculate the critical Reynolds number and gap width for antiphase oscillations 2.34 times the cylinder diameter. Not only this but when the gap width is

smaller than this critical value, an in-phase oscillation is observed, although the cause of this oscillation is still unknown.

Flow around cylinders has been a fundamental problem in fluid mechanics due to its wide range of applications in engineering fields such as structural design, offshore structures, heat exchangers, and aerodynamics. Understanding the flow pattern characteristics near the cylinders, particularly in rotation, has the potential to revolutionize the reduction of drag and suppression of vortices. This review of relevant literature presents the extent of research on drag reduction and vortex suppression in the near wake flow of two counter-rotating and closely spaced cylinders and its relation to rotational speed and aspect ratio on flow patterns and heat transfer.

1.2.1 Flow Around Rotating Cylinders

Another study on fluid dynamics and heat transfer of a tandem of two cylinders was conducted by Darvishyadegari and Hassanzadeh in 2019. In their work, it was indicated that the rotational speed and interval between the cylinders exert a major influence on the transformation of flow patterns and heat transfer behaviors. There were changes in the recirculating zones, location of the front stagnation points (where the flow separates) and negative lift forces with the increment of the rotational speed and gap distance. The study also showed that the shed rate reduced with the rise of the rotational velocity, this approached the equal distribution of the heat transfer on both cylinders. The large eddy simulation approach was used in the investigation of the vortex shedding by Karabelas in 2010 for a single rotating cylinder. His findings indicated that the advancing lower vortex had a diminishing size and eventually lost; thereby the drag decreased. Strategies that break the formation of a shed are relevant for applications requiring steady conditions flow, including aerodynamics and heat exchangers. Finally, experimental tests were also conducted by Dol, Kopf, and Martinuzzi in 2008 to analyze the vortex shedding around a rotating cylinder. They have maintained the experiment conditions at Reynolds 9000. It was established that under non-dimensional rotational speed of 2.7 the drag reduced. The findings imply that the consequences of varying the rotation of the cylinder could be significant.

1.2.2 Vortex Shedding and Drag Reduction

Vortex shedding and the accompanying drag forces are two significant factors that must be considered by fluid dynamics experts, particularly when dealing with cylindrical objects. Although some effort can be taken to prevent fluid from lapping in certain directions around a object, it is possible guarantee that the object does not form revolving patterns of fluid. As a result, it is probable to decrease the drag involved and increase the structural support provided. According to Lam, a slowly rotating circular cylinder develops key fluid dynamic ramifications which influence drag and lift. The aforementioned study examines the speed of rotation, which is increased and showed that the quantity of vortices diminishes and the totality of time it takes for it to generate is considerably less, making drag reduction easier. Another study that has been examined in the past is that by Rao et al.. The researchers examine the flow around a rotating cylinder that is placed at varying distances from a wall. The incorporation of clockwise and counter-clockwise rotations is also discussed. The most interesting is full vortex suppression when rotation is performed in a reverse manner. This research provides additional insights into flow structure control, which can be utilized to reduce drag and eliminate the vortex entirely.

1.2.3 Heat Transfer in Rotating Cylinders

On considering the stationary case, one can say that the heat conduction behavior is influenced by the tube's angular velocity and flow conditions. The source of the publication by Ghazanfarian and Nobari is a numerical analysis that explains how an oscillating rotating cylinder with its axis perpendicular to the flow convects heat. Contrary to unidirectional study, increasing the rotation velocity will reduce the rate of heat transfer. Paramane and Sharma also researched this particular case. The scientists performed heat conduction and fluid flow around a rotating cylinder with a constant heat flux. On increasing speed, the expected strength of vortices will decrease and, therefore, the Nusselt number will also diminish. The findings of the investigation have significant fundamentals to understand the thermal conduction of tubes that are rotating and exposed to flow.

1.2.4 Effects of Cylinder Arrangement

Vakil and Green used a study aimed at flow patterns around two circular cylinders next to each other under conditions of moderate flow, the results illustrate a complex process regarding the interaction between the cylinders wake and its effect on drag and lift.

Elhimer et al. focused on the organized and disordered behaviors in the bistable regime of a pair of cylinders, and high-speed PIV data. They also aimed at reattached flow dynamics.

1.2.5 Fluid Dynamics and Numerical Simulations

The work of Patankar that described fundamental techniques in numerical heat transfer and fluid flow is very important today for works with computational fluid dynamics. This is determined by the fact that most of the studies to date use these methods to simulate and analyze the effect of any factor on heat transfer and flow dynamics. The mathematical model of the flow passing by a circular cylinder was developed using an unsteady panel method by Ramos-García et al. It demonstrated the three-dimensions of the wake and how they act on the inhibition of the vortex and drag.

1.2.6 Experimental and Computational Studies

Experimental studies are also extremely important in validating computer models and real-world data against a developed numerical simulation. For instance, in 2014, Stringer, Zang, and Hillis conducted an experiment when comparing several unsteady Reynolds-Averaged Navier-Stokes calculations of the flow around a circular cylinder. The method offered by those authors also contributed to explaining the flow's patterns, and the examination of several drag reduction methods explored for decades showed some leveling of the process. Another experimental study replicating numerical simulations was conducted by Rajagopalan & Antonia in 2005. They investigated the structure of the flow in a developing mixing layer of the near wake of a circular cylinder testing stable and unstable modes of this layer with reduced drag forces.

1.2.7 Low Reynolds Number Flow Characteristics for Two Side by Side Rotating Circular Cylinders

The study examines the complex flow dynamics between two rotating circular cylinders running side by side at low Reynolds numbers. It seeks to inform on the implications of these properties on vortex generation and vortex shedding and the overall behavior of the flow based on the different levels of rotation and gap ratio. The investigation includes the use of sophisticated numerical simulations to present an adequate apprehension of fluid behavior involving the configuration in question. The study's major findings include the identification of multiple flow regimes that appear at different rotational levels and Reynolds numbers. While the flow is mainly laminar and uniform at low Reynolds numbers with symmetric vortex patterns, the situation is unstable with periodic vortex shedding and intricate, turbulent wake interaction as the Reynolds number increases. Similarly, the research underlines the stabilizing influence of cylinder rotation on flow through the explanation of the impact of the rotating speed of the cylinders on the critical Reynolds number under which the shift takes place. A computational fluid dynamics software served in the simulation of the flow around the cylinders. A fine mesh was used in the simulations; thus, allowing for the capture of the intricate flow field characteristics. Measurements were taken over a variety of rotation rates, from zero to a fast-spinning rate, in both cylinders in order to establish the subsequent changes on the flow patterns. The gap ratio was also varied to study the subsequent impact on wake dynamics and vortex interaction.

The study has a variety of interesting findings. The flow is stabilized by the rotation of the cylinders at low rotational rates. It delays the velocity at which vortex shedding starts and causes lower drag. As a result of being subjected to the centrifugal forces induced by the rotating cylinders, which modifies the pressure distributions surrounding the cylinders, the causes for this degree of stability are absent. However, more wakes are paired and a variety of source shedding modes are present in the flow at larger rotational rates. It is important to investigate the dragging forces involving the pressure distributions across the cylinders. The data appears to be consistent with the reality, and the drag force on the cylinders shifts position as a feature of the rotating rate. As seen, large changes occur within the pressure

coefficients over the cylinder surfaces. The modifications are thoroughly and using documented, statistical data, the study provides valid data and insights surrounding the more appropriate uses of rotational flow to minimize drag forces. The findings of the study have a variety of applications. Flow properties around rotating cylinders are advantageous when constructing rotors, turbines, and other spinning machines. The information on enhancing the drag coefficient can also be used by engineers to create systems that utilize this type of dynamic to control drag and enhance the efficiency of technical systems. All in all, this work deepens knowledge about the phenomena of low Reynolds number flow revolving cylinders. The data is comprehensive and analyzes each of the impacts in rotation dangers.

1.2.8 Control of Vortex Shedding from Two Side-by-Side Cylinders

This study explored the mechanics of control of vortex shedding between two side-by-side cylinders using different rotating structures. The goal was to determine how different rotational speeds and positions can influence the possibility of vortex suppression and drag reduction. The results of such a study are highly relevant to fluid dynamics and systems design in which vortex shedding is a major concern. These include heat exchanger tubes, offshore exertions, and bridge piers. Vortex shedding is a typical phenomenon when the fluid passes a bluff body, and the system creates alternate vortices in its wake. In general, these vortices instigate oscillatory forces in the system, influencing vibrations and then the fatigue of the system itself. Therefore, maintaining the assistance for vortex shedding is important considerations in the stability and endurance of the componentized systems to the fluid flow. Meanwhile, this paper examines the flows over two parallel cylinders using various devices such as numerical and experimental methods. For the experimental set up, a wind tunnel is used as the experimental set up at which both cylinders are placed next to each other and fully spun at various speeds. Apart from the vortex patterns allocations, the flow velocity fields are analyzed using the flow visualization techniques such as the Particle Image Velocimetry techniques. The application of the numerical approaches enhances the obtained commercial results regarding the understood flow field dynamics and the allocation of the pressure fields over the rotating cylinder using the full variables. Therefore, the most important observation is choosing the most recommended cylinder

rotating configuration at which shedding is minimized. From the results, it can be calculated that the dragging coefficient can be drastically reduced if both cylinders spin simultaneously at contingencies. Therefore, the outcome suggests that the simultaneous rotation at the full variable speed is impressive in the suppression of the vortex shedding. Finally, the results contain the images produced over the observation of the flow indicating the shed vortex and then the non-shed vortex produced over the cylinders.

The second main conclusion of the study is the consequences of counter-rotation of the cylinders. Counter-rotation at distinct speeds and their gap ratio introduces many flow regimes due to the complicated connection between the vortices generated from each cylinder. The study concludes that depending on the gap ratio and the relative rotational speeds between the two cylinders, counter-rotation may enhance or reduce the vortex shedding. The drag forces and pressure distributions are thoroughly investigated to understand the underlying mechanism in both of these cases. The results of these findings for practical usage are well addressed in the study. For example, controlling the vortex shedding can increase the efficiency of heat transfer and vibrations in heat exchanger system design. In such a design, several tubes are installed side by side and thus may benefit from the investigation for the most efficient rotating configuration, hereby boosting the life and efficiency of the exchanger. Overall, this study extensively investigates vortex shedding control between two side-by-side cylinders with rotational structures. The use of numerical and experimental methods provides an excellent overview of the process of vortex suppression and vortex formation. The results have various applications in fluids science and engineering, especially in systems design in which vortex shedding is critical.

1.2.9 Effect of Rotational Speed on the Stability of Two Rotating Side-by-Side Circular Cylinders at Low Reynolds Number

This work investigates the effect of varied rotational speeds on the flow stability and vortex formation behind two side-by-side rotating identical circular cylinders at low Reynolds numbers. The experiment is used to examine how different rotations per minute of the cylinder affects the occurrence of vortex shedding, flow stability, and drag on the bodies. The results of this paper come in handy in the engineering departments, where minimizing

the influence of drag on bodies flow by vortex-induced is the main concern with the given results about the required RPMs to mitigate it. The research used numerical simulations and theoretical analysis to understand the various mechanics involved. The numerical approaches are high-resolution computational fluid dynamics simulations with high-resolution to capture the small-scale flow disruptions by the rotating bodies. Most often used rotational speeds are sought while varying the properties of the gap for observation. Here are the key outcomes of the investigation: the research found out how a critical RPM exists beyond which the flow becomes unstable. As the revolving speed increases from low to high, the flow remains laminar and symmetric with the same vortex patterns behind the objects. At high RPMs, the flow dissipates these patterns in an unsteady pattern through intermittent vortices. It has provided evidence on the critical RPMs for intake and Reynolds number specific. The paper has also presented the findings of the outcome of pressure distribution pressures and drag. The introduction of pressures changes the surface on the cylinders, which results in drag changes. It has been quantitatively presented with the displays of plots for the pressure coefficients. The research has also discussed the consequent tendencies on drag in similar displays, providing how drag can be controlled by rotational speed. The wake dynamics and vortex preparation between the objects under varied RPMs' have been discussed. The results show how the rotational values affect the vortex's strength and the number shed from the rotating cylinder.

1.2.10 Numerical Investigation of Flow Across Three Co-Rotating Cylinders

The present paper expands the study of fluid dynamics on a system involving three corotating cylinders. More specifically, this research aims to discover how the addition of the third cylinder to the two existing ones alters the flow pattern, vortex dynamics formation, and drag forces. This study is important since it can be directly applied in various engineering domains. For example, heat exchangers commonly consist of multiple cylinders closely placed next to each other. This research incorporates advanced numerical simulations of fluid flow around three cylinders based on computational fluid dynamics tools. These simulations allow obtaining detailed information on vortex interactions and complex fluid flow patterns that occur under these circumstances. The experimental analysis is held on various combinations of rotational speeds and gap ratios between the

cylinders. The obtained results demonstrate various regimes of flow depending on the rotational speed and relative position of the cylinders. The distinctive patterns found in this study include steady symmetric flow at low rotational speeds and unsteady asymmetric wake regimes at high velocity. Furthermore, the paper elucidates the changes in vortex dynamics due to the presence of the third cylinder. It found that the third cylinder notably alters the flow patterns in all regimes. Depending on its rotational speed and the relative cylinder positions, it can both stabilize and diminish the flow. The results are shown using the calculated velocity fields illustrations.

The study also examines the pressure distribution and drag forces on the cylinders. It is evident from the results that the pressure coefficient varies from adding the third cylinder on the faces of the cylinders, which also results in different drag combinations. The results elaborated in the study compile sufficient data regarding the same, and it is instrumental in showing how the combination of the arrangement like the min or max speed rotation make minimizes the drag for less pressure. The heat transfer in the three-cylinder configuration is also part of the research options assessed. In the three-cylinder configuration, the heat transfer rates are determined through the use of the rotation speed and the spacing as analyzed in the simulation modules. The outcome results indicate that there are specific cylinder configurations that can be used to improve the heat transfer, which is impact-oriented for heat exchangers and other thermal integrations. The study will have vast applications and implications, and these include the design and optimization of different engineering configurations with multiple rotating cylinders. There will be no limitation of the engineering system as the information and analysis, as discussed in the paper, provide a bigger scope for the study and research endeavors. Finally, overall the paper was a detailed numerical examination about the flow over three co-rotating cylinders. The findings give vital information about the complicated flow dynamics of the vortices in multi-cylinder locations. These findings have great value on the industry scale as the design and optimization benefits are vast, as well as the heat transfer study for plants and other systems.

1.2.11 Effect of Counter Rotation on Fluid Flow and Heat Transfer

The team focuses on studying the contours of counter-rotation circularly oriented cylinders through the examination of fluid dynamics. More specifically, the research aims to establish how the use of counter-rotation does to the general flow conditions, vortex patterns, and heat transfer rates. The findings of the study may be welcome to future reclamation given the current need for optimal fluid dynamics in engineering systems seeking to enhance performance regarding flow control and heat transfer characteristics. The team relies on a combination of simulations and experimentation techniques to establish the flow patterns of the counter-rotation of cylindrical components. The simulation employs recent computational fluid dynamics methods to have a clear picture of the flow pattern under examination. The experimental environment entails a water tunnel where the cylinders' orientation is modified to counter-direction rotation while also varying the velocity of flow enabling the video recording of flow behavior. A second finding is related to the stability of fluid contours under this framework. The team also established that the counter-rotational framework creates new contours characterized by steady unobstructed vortexes alongside the two disks while variability is noted when the rate of augment is factor every cycle. This paper develops velocity patterns alongside simulations and coupled velocity scrolls to help further understanding. The assessment also investigates counter-rotational patterns influence of pressure as well as its impact of drag force. This study reveals a substantial difference in the coefficient of pressure and drags force created under counter-TOR rotation, while it notes that there is a linear correlation with the counter-rotational approach. Another significant detail is that it is possible to use the available data to get an idea of the pressure coefficient and use that to derive the drag force generated. Other study areas in this regard investigate the effect of counter-rotations in transferring of heat. This study found a substantial rise in transferred heat due to a mixture of pressure that is generated and the disruption of the thermal boundary layer. This study reveals that the best approach to reflecting a counter-rotational approach to alleviate pressure force effects is an advantageous technology. Minimizing drag force will drive flow speed. This study has extensive implications as it might see stress reduction effective on cylinder use. The foundations of this study are partly weak.

1.2.12 Vortex-Induced Vibrations of Two Mechanically Coupled Circular Cylinders

The present paper investigates the problems related to the vortex-induced vibrations of two circular cylinders mechanically coupled to each other. VIV is a phenomenon in which vibrations of structures arise from oscillatory forces due to identical vortex deformation leading to destruction of the structure in most cases. Mechanically induced vibrations can disrupt the smooth functioning of many civil structures, including bridges, offshore platforms, and even heat exchanger tubes. Therefore, understanding VIV is a vital concern when analyzing real industrial machines exposed to the action of surrounding fluids. The paper investigates these issues using combinations of experimental studies and numerical simulation of VIV. The experimental setup is made in the form of a wind tunnel in which the studied cylinders are attached. Cylinders are connected to a mechanical coupling using a rigid link or springs determining their mechanical interaction. The VIV process is tracked by the attached high-precision vibration sensors. Numerical simulation and computational data provide comprehensive information about flow parameters, tracking all the vortex interactions surrounding the cylinders throughout the experiment. The study makes a relevant contribution by showing that the mechanical coupling of experimental cylinders significantly affects their VIV activity. The degree of vibrations and their occurrence changes depending on the ratio of the stiffness of the link between the cylinders and the fluid parameters. The paper provides a variety of patterns for coupling and optimal stiffness that shows the obtained measurements of vibration parameters, which increases the understanding of the physical processes under study. The work further analyses the effect of VIV on the flow and vortices shed from the cylinders. The studies through numerical simulation show a complex pattern of interaction with multiple flow modes caused by vibration. It has been found that the vortex shedding becomes synchronized or desynchronized under certain flux conditions. The paper demonstrates visualized data and measured velocity fields. The inverse problem of VIV is analyzed in this paper by calculating new coefficients of pressure on the surface and draft factors. The measurements show that the pressure on the surface changes in response to the vibration, which affects the draft forces. The paper shows the overall data on the measured pressures, which will make it possible to apply knowledge about VIV to control the draft forces and the mechanisms of stability of the structure. Thus, it is necessary to note as a practical result

of the work that all studies have implications for the practical design of structures. VIV has been well studied for a single cylinder, but the mechanism radically changes when considering several cylindrical layouts. Therefore, obtaining an amplitude-frequency graph for such a system and visualizations of flow fields is practical knowledge for the development of structural units. To conclude, the present paper provides a detailed analysis of the VIV process of mechanically interconnected in two circular cylinders. All combinations of works, experimental and numerical, can fully explain the phenomenon and its effect on the flow and stability of the structure. It is also possible to note the industry-related implications of VIV work due to the availability of quantitative studies and data.

1.2.13 Flow Interference for VIV Responses of Adjacent Cylinders

This paper studied the effect of flow interference on the VIV responses of two adjacent cylinders. In the natural vibration of a single cylinder, the vortices coming off the cylinder are not great and do not interact with other vortices created by a different cylinder. However, the out shedding fields can interact with each other when the cylinders are in proximity. Therefore, the effects of flow and interference between the two cylinders must be closely monitored and well understood to contribute more to coseismic structural designing and safety of the many structures facing the experience of fluid flow, including heat exchangers, offshore platforms, and bridge piers. To achieve their purpose, the authors utilized both experimental and numerical methods considering a cluster of two cylindrical spars. The space between the elements was varied, and the installed scales inside the tunnel were activated. The flow over the cylinders was visualized using high-speed cameras, and PIV measured the velocity fields. The numerical method was used to supplement the obtained results by providing more insights into the pressure distributions over different flow cases and the effects of interference by defending the structures. The primary result of the paper is how flow interference affects the VIV response of two adjacent cylinders. Depending on the interval and flow speeds, it can either increase or reduce the VIV reaction. The paper also offered measurements of the VIV amplitude and frequency value for different intervals and flow speeds, suggesting a possible explanation for what causes the effect. The paper authors also explored the effect of flow interference on the vortex-

shedding frequency. Their simulations data show that the presence of an adjacent cylinder altered the vortex shedding frequency, resulting in synchronization or de-synchronization, depending on the cylinder's interval. For example, at a small interval, the vortices interact and are synchronized in shedding; hence the VIV gets more intense with low intervals.

NUMERICAL MODELING

2.1 Introduction

An unsteady flow varies in time in either a random or periodic manner. Both need to be adequately addressed to predict the correct performance of the turbomachines. Two main features are associated with the unsteady flow phenomena. First is the aerodynamic performance related to the blade row interaction and flow instabilities such as stall and surge. Second is the blade's structural integrity when it undergoes flow-induced vibrations, i.e., forced response and flutter. In this study, we have simulated the aerodynamics of a one-and-a-half-stage axial turbine and computed aerodynamic loads for performing forced response of uncoated and coated turbine blades.

2.2 Navier Stokes Equations

2.2.1 Introduction

The Navier-Stokes equations are critical to fluid mechanics, where fluid substances are materials that move such as liquids and gases. Fluid dynamics rely on the conservation of mass, momentum and energy require an orderly, formal language to comprehend and define a wide spectrum of phenomena. The two-dimensional Navier-Stokes equations are also an essential instrument used frequently in practice, including aeronautics and on weather models and oceanic flow. This paper provides an in-depth description of 2-D Navier-Stokes equations, their derivation and fluid dynamics importance.

2.2.2 Derivation of the 2-D Navier-Stokes Equations

Continuity Equation

The continuity equation for a two-dimensional incompressible flow is given by:

$$\partial u / \partial x + \partial v / \partial y = 0$$

This equation ensures that the mass of the fluid is conserved as it flows.

Momentum Equations

The momentum equations in the x and y directions are given by:

$$\rho(\partial u/\partial t + u\partial u/\partial x + v\partial u/\partial y) = -\partial p/\partial x + \mu(\partial^2 u/\partial x^2 + \partial^2 u/\partial y^2) + f_x$$

$$\rho(\partial v/\partial t + u\partial v/\partial x + v\partial v/\partial y) = -\partial p/\partial y + \mu(\partial^2 v/\partial x^2 + \partial^2 v/\partial y^2) + f_y$$

Physical Interpretation

The 2-D Navier-Stokes equations encapsulate several key physical phenomena in fluid dynamics

- **Inertia:** The terms $u\partial u/\partial x$ and $v\partial u/\partial y$ (and their counterparts in the y-momentum equation) represent the convective acceleration of the fluid, reflecting the change in momentum due to the fluid's motion.
- **Pressure Gradient:** The terms $\partial p/\partial x$ and $\partial p/\partial y$ denote the influence of pressure differences within the fluid, driving the fluid motion.
- **Viscosity:** The terms $\partial^2 u/\partial x^2$ and $\partial^2 u/\partial y^2$ (and their counterparts) account for the viscous forces within the fluid, which resist the fluid's motion and cause dissipation of kinetic energy.
- **External Forces:** The terms f_x and f_y represent any external forces acting on the fluid, such as gravity or electromagnetic forces.

Solution Methods

It is not possible to solve Navier-Stokes equations analytically due to the nonlinearity of the equations and the coupling between the components. Therefore, numerical methods are required to approximate the solution. Some of the most popular numerical techniques are:

- **The Finite Difference Method :** The simulation space is divided into a grid, and finite difference approximations are used to estimate the relevant derivatives. Although simple, it is easy to implement, but could lead to stability and accuracy issues with complex flows.

- The Finite Volume Method : In FVM, the simulation space is divided into control volumes, and conservation principles are applied to them. Since FVM well conserves of the fluxes at the CV boundaries, it is often used for Computational Fluid Dynamics simulations.
- The Finite Element Method or FEM: In FEM, the simulation space is split into elements via boundaries. The general results are calculated based on the value of the results at the boundaries.
- Spectral computations: In spectral techniques, the solution is recovered as the sum of the analytical basis functions. The equations are solved in the compact space that describes the spatial variability. It is computationally costly but very precise; smooth problems are stereotyped.

Applications

The 2-D Navier-Stokes equations are applicable in various fields, including:

- Aerodynamics: Studying the flow over airfoils and around obstacles to optimize the design of aircraft and automobiles.
- Meteorology: Modeling atmospheric phenomena such as weather patterns, cyclones, and turbulence.
- Oceanography: Understanding ocean currents, wave dynamics, and the dispersion of pollutants in marine environments.
- Biomedical Engineering: Simulating blood flow in arteries and around medical devices to improve healthcare outcomes.
- Industrial Processes: Optimizing processes such as mixing, chemical reactions, and heat transfer in engineering systems.

Challenges and Advances

Despite their wide applicability, solving the Navier-Stokes equations remains challenging due to several factors:

- **Turbulence:** Turbulent flows are characterized by chaotic and unpredictable behavior, making them difficult to model accurately. Advanced turbulence models and large eddy simulations (LES) are employed to tackle this issue.
- **Boundary Conditions:** Accurate representation of boundary conditions, especially for complex geometries, is crucial for obtaining reliable solutions.
- **Computational Resources:** High-resolution simulations require significant computational power and resources. Advances in parallel computing and GPU-based simulations are helping to address this challenge.
- **Multiphase Flows:** Simulating flows involving multiple phases (e.g., liquid-gas or solid-liquid) adds complexity due to the interactions between different phases. Specialized models and numerical techniques are being developed to handle such cases.

The governing equations for the fluid flow employed in the current research are incompressible Navier Stokes Equation below.

$$\rho \cdot ((Dv^{\rightarrow})/Dt) = -\nabla p + \nabla \cdot T + f^{\rightarrow}$$

The flow around the cylinders is simulated using the Finite volume method. The flow governing equations are discretized using ANSYS Mesher. The SIMPLE algorithm solves the pressure correction equation to achieve mass conservation. The methodology adopted for this research is further summarized in Figure 0-1

2.3 Computational Domain and Boundary Conditions

The flow is assumed to be incompressible and laminar. The cylinders are considered to be perfectly smooth. At the inlet, a constant uniform velocity is applied with streamwise and transverse components as $u = 0$ and $v = 0$, respectively. The velocity and pressure gradients at the outlet are set to zero. Symmetric boundary conditions are applied to the top and bottom boundary conditions, implying that there is no flow perpendicular to these boundaries, and the flow parallel to these boundaries is solved using a momentum equation. The flow is simulated for a range of rotational speed boundary conditions applied at the two downstream cylinder surfaces. At a specified Reynolds number, it is defined as Re

where $Re = \rho U D / \mu$, where U is the free-stream velocity and μ is the kinematic viscosity of the fluid. The non-dimensional rotational speed of the downstream cylinders is denoted by α . The flow is assumed to be fully developed. The flow is simulated for a range of cylinder spacing, $g^* = g/d = 0.5, 1, \text{ and } 3.0$. The flow is simulated for a range of non-dimensional rotational speeds, $\alpha = 0 - 5$, with increments of 0.5. The computational domain is discretized using a structured grid. The grid is generated using the ANSYS Mesher. The flow configuration of interest is shown in the figure. A rectangular computational domain with a height of $31.5 d$ and a width of $100 H$ is used for this study. The non-dimensional time step $t^* = \Delta t U / d$ for this case was 0.002. The downstream cylinders are rotating with a constant angular velocity ω . The computational domain for the current study is shown in Figure 0-2.

2.4 Mesh Independence Study

A mesh independence study was conducted to analyze the impact of mesh density on the accuracy and reliability of the numerical results. The research utilized a structured mesh, which was specifically designed to ensure consistency and precision in the simulations. The cell size within the mesh was carefully chosen to achieve a high level of detail, particularly around the boundary layers of the cylinder surfaces being studied.

To achieve this, the mesh was refined to ensure that there were at least 10 to 15 grid points within the boundary layer on each cylinder surface. This level of detail was critical in capturing the complex flow phenomena and ensuring that the numerical results were not overly dependent on the mesh density. As a result of this meticulous mesh design, the study obtained a total of 25,000 grid points and 45,000 elements.

The study also focused on the mesh distribution in the vicinity of the three cylinders, where accurate resolution of the boundary layers is essential for reliable simulation outcomes. The structured mesh was employed to provide a uniform and systematic grid distribution, which is advantageous for minimizing numerical errors and enhancing the convergence of the results.

Moreover, an additional mesh independence analysis was performed to further explore how variations in mesh density might influence the numerical findings. In this part of the investigation, the cell size was adjusted to ensure that each cylinder surface had a minimum of four to five grid points within the boundary layer. This approach allowed the researchers to determine the optimal mesh density that balances computational efficiency with the accuracy of the results.

Overall, the mesh independence study played a crucial role in validating the numerical simulations by ensuring that the results were not significantly affected by the choice of mesh density. This thorough investigation contributed to the robustness and reliability of the computational analysis, providing confidence in the findings derived from the structured mesh approach.

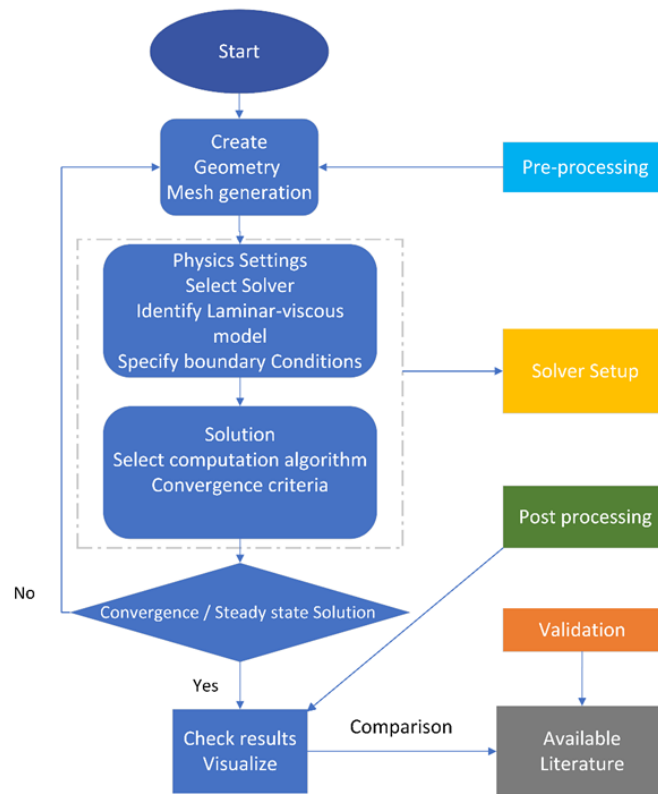


Figure 0-1 Methodology

The computational domain consists of two cylinders arranged vertically. The Diameter of each cylinder is d , and the surface-to-surface distance is denoted by g .

The cylinders measure 25 diameters upstream and 75 diameters downstream from the inlet and outflow, respectively. The vertical boundaries on either side of the cylinders measure 31.5 diameters.

There were 25000 grid points and a total of 45000 elements collected. The Figure 0-6 Depicts the mesh near the two cylinders.

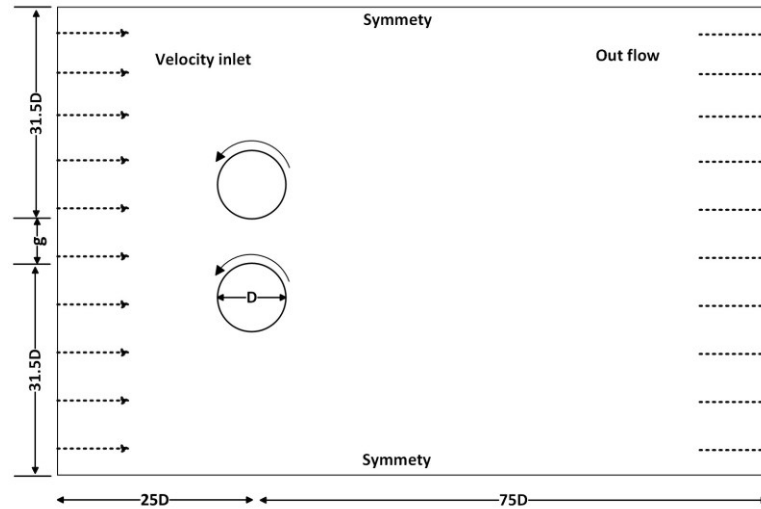


Figure 0-2 Computational domain for the flow

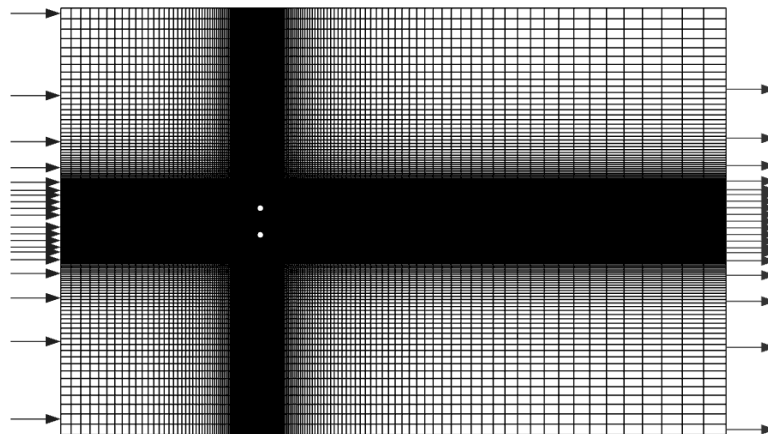


Figure 0-3 Structured Mesh used in this study

2.5 Numerical Method

The proprietary software ANSYS Fluent is employed for the creation of the CFD model. Fluent is a widely used computational fluid dynamics (CFD) software that has been engaged in numerous studies investigating the flow around cylinders. The model used in this case is laminar. This model has demonstrated efficacy and has been commonly utilized in previous studies on the flow around cylinders.

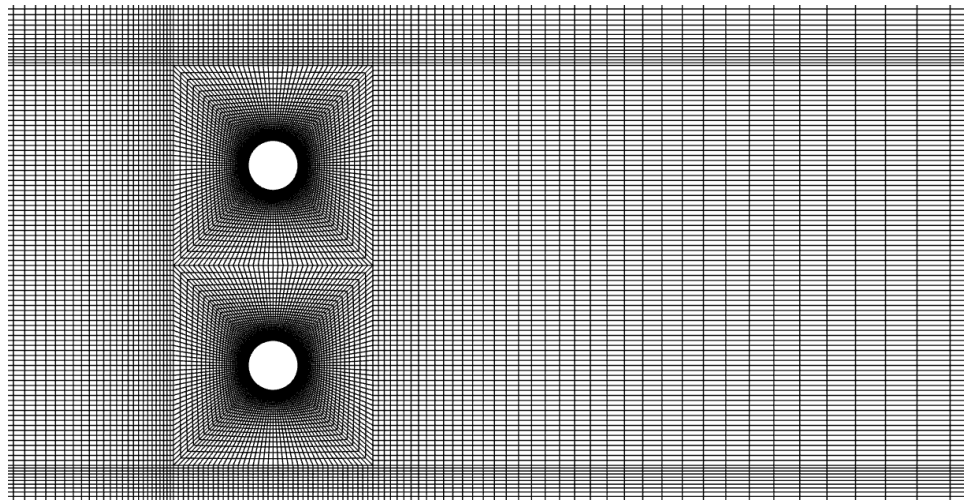


Figure 0-4 Optimal mesh close up view

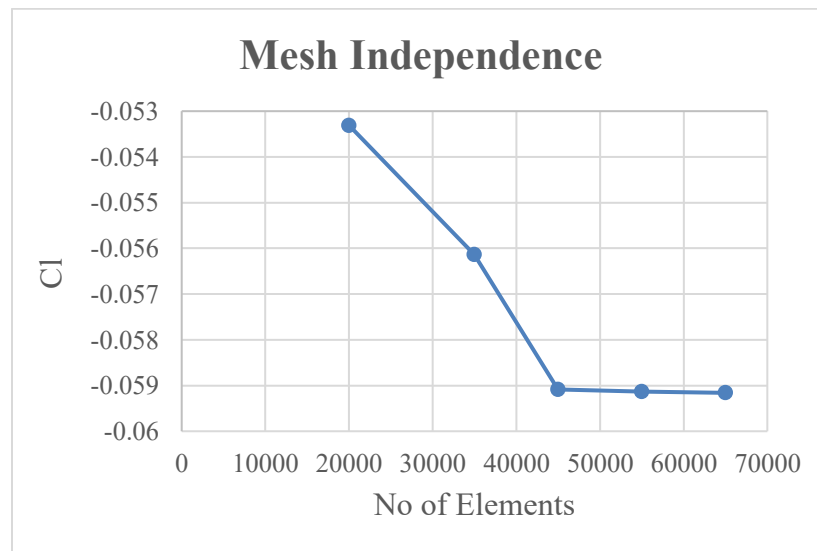


Figure 0-5 Mesh Independence Study

2.6 Validation Case

The numerical technique has been successfully validated for a configuration involving cylinders arranged side by side, with a gap spacing denoted by g^* of 3.0. The study specifically considered a range of non-dimensional rotational speeds, from 0 to 5, for the downstream cylinders, which were subjected to counter-rotational motion. Additionally, the flow conditions were characterized by a Reynolds number (Re) of 150. This validation confirms the effectiveness of the numerical approach in capturing the complex fluid dynamics associated with these specific configurations and conditions.

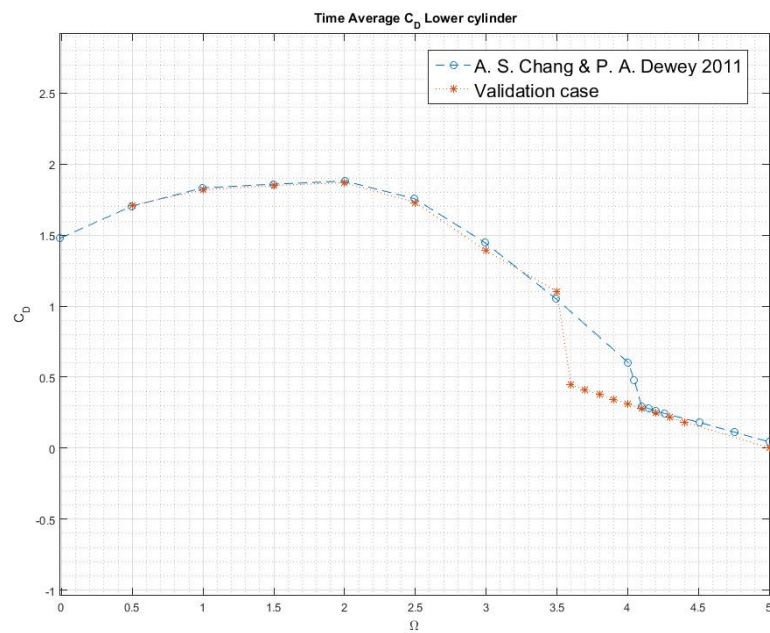


Figure 0-6 Validation Case

Table 1 Validation results

Critical Speed	(Experimental	Validation A.S Chan et. Al 2011	This study
α_{crit}	3.71	4.11	3.6

The comparison is shown in Table 1. The above table depicts that the predicted results are in complete agreement with Chen et al. (2011), validating the numerical scheme used in the current study.

RESULTS AND DISCUSSION

3.1 Introduction

The findings of the numerical study presented in this unit center around the flow solution of the flow dynamics surrounding two vertical, and identically rotating cylinders close to each other. The highly constrained flow problem is analyzed carefully, taking into account the many interplaying influences on the flow field. The complex scenario of the flowing intimately close to the stationary center lines of two identically spinning cylinders leads to various phenomena, mostly based on the interaction of the wakes. The wakes can be identified by pairs of opposite rotating vortices, flow structures of specific size and scale. The size of the vortices is directly a function of the size and rotational of the first cylinder, called the Reynolds number, along with the rotation frequency of the cylinder, and the diameter of the two cylinders. The rotational effect of the first cylinder acts on the flow immediately behind the second cylinder, causing a Coriolis effect that enhances the overall circulation, which becomes stronger with a higher turning frequency. The separation between the cylinders has a moderating effect on the circulation since a more considerable separation will result in larger vortex formation due to a higher rate of contact with the wakes. The turning of the two spinning cylinders creates a visible pressure gradient around them which is enhanced further with more increased turning. CFD simulations permit detailed observations of flow patterns, wake structures and their interaction, and the simultaneous effect of various influences on the overall flow characteristics.

3.2 Flow Structures

The figures below depict the flow patterns for various cylinder spacing values, specifically $g^* = 0.5, 1, \text{ and } 3$. They also show the flow patterns for non-dimensional rotational speeds ω for values of 0, 0.5, 1, 1.5, 2.0, 2.5, 3.0, 3.5, 4.0, 4.5, and 5.0.

3.3 Wake Structures

The diagram depicts the observed wake structures as the lengths between each cylinder change. The turbulence due to each cylinder increases as the lengths between the cylinders

become more extensive. As expected, since the cylinders' connection to the flow generates the wake, when the cylinders are further apart, they generate less fluid after their disruption away. As a result, the cylinders may move further apart and interact with one another in an independent manner.

3.4 Effect of Cylinder Spacing

The distance between the gaps is of fundamental importance in creating the vortices. The configuration of the created vortices can also be dependent on the distance between the gaps and its dimensions. Cylinders with a smaller gap distances will create a single vortex as all the created vortices join. This is in contrast to wider distances, which have entirely separate vortex sheets around the cylinders. The distance between the gaps also affects the number of vortices created. The larger the gap separation, the more the vortices stop synchronizing. A smaller gap separation will reduce the synchrony, while a larger distance will increase the total number of vortices. The distance between the gaps will also affect the shape of the vortex created. A smaller gap will create a more uniform, circular shape, while a larger gap will be more elongated.

3.5 Effect of Rotational Speed

The angular velocity of the cylinder has a strong direct and many indirect impacts on the creation of vortices in the fluid flow. The most direct way to change the course fluid particles would be the Coriolis force, which deflects the fluid from its starting path. The strong force correlates to the cylinder's angular velocity and the fluid's velocity and its increase with the cylinder's angle results in change of fluid's velocity path and the formation of vortices. The cylinder's rotational pace indirectly influences the creation of vortices through the pressure gradient. The pressure gradient is the difference in pressure of the fluid inside and outside of the cylinder is the difference. The force pushes the fluid in an outward direction to the cylinder based on the rate of change of pressure across it.

3.5 Discussion

3.5.1 Gap Ration of 0.5 ($g^* = 0.5$)

As stated, our study was focused on the wake interactions of co-rotating side-by-side cylinders. The studied gaps were those of 0.5, 1, and 3, and the Reynolds number was tested at $Re = 50$ and $Re = 100$. The rotation of cylinders resulted in unique interactions between the vortex streets generated in their wakes. Specifically, the wake interactions determine the level of rotational rates required to stabilize wake instabilities. When the gap increased from 0.5 to 3, the interaction diminished. Given that the vortex streets interacted less when the gap increased, a critical rotational speed was required to stabilize the wake instabilities effectively. However, the outcomes of this study suggest that relatively low rotational speeds of $\alpha_{crit} > 3.5$ are sufficient to stabilize the wakes. A simple analogy could be two cylinders next to one another and rotating in water before them. The wake of the cylinders will have different instabilities; however, the research indicates that irrespective of the gap space, the rotational effect maintains the stability. It could mean that even at larger spacing, increased rotation would stabilize the wake. However, this should be further analyzed and demonstrated.

Consider the case at $Re = 50$. For all rotational speeds below the critical speed of $\alpha_{crit} = 3.5$, we observed stable anti-phase drag coefficients for the cylinders. The time histories indicated that the lift forces on both cylinders were in phase. The average drag coefficient for the upper cylinder increased as the rotational speed increased, reaching a maximum peak in drag at $\alpha = 2$, after which it decreased again with further increases in speed. In contrast, the drag coefficient for the lower cylinder decreased with increasing rotational speed until reaching the critical rotational speed, at which point it began to increase. Notably, at the critical speed, the drag coefficient for the lower cylinder turned negative, implying that the cylinder was generating thrust instead of drag.

The situation exhibited a different behavior at $Re = 100$. For rotational speeds less than $\alpha < 1.5$, the anti-phase drag coefficients were unstable. However, the vortex street remained stable and continued to be stable until $\alpha_{crit} = 3.5$, beyond which the vortex street diminished,

with no secondary instability observed up to a rotational speed of 5. This indicates a shift in the stability characteristics of the system as the Reynolds number increased. At $Re = 100$, due to the unstable vortex shedding mode, there was a noticeable variation in both the lift and drag coefficients. Despite these variations, the drag coefficient for both cylinders followed a similar trend to that observed at $Re = 50$.

However, the lift coefficient's behavior differed significantly at $Re = 100$. For the upper cylinder, the average drag coefficient increased with rotational speed, peaking at $\alpha = 2$ before decreasing as the speed continued to increase. For the lower cylinder, the drag coefficient decreased with rotational speed up to the critical speed, where it then began to rise again. At the critical rotational speed, the drag coefficient for the lower cylinder once again turned negative, indicating thrust production. The lift coefficient showed minimal variation for the upper cylinder, but for the lower cylinder, it increased, suggesting more complex dynamics at play, particularly under the unstable vortex shedding mode observed at higher Reynolds numbers.

An intriguing phenomenon observed during the study was the behavior of small eddies in the co-rotation scenario, where both cylinders exhibited eddies moving in the same direction. In contrast, in the counter-rotation case, these small eddies moved in opposite directions. This difference in behavior can be attributed to the adverse pressure gradient induced by the rotating cylinders.

The no-slip condition at the cylinder surfaces led to a higher pressure at the top of each cylinder and a lower pressure at the bottom. As the cylinders rotated, the fluid, moving along with the cylinders, encountered this adverse pressure gradient. This interaction caused the fluid to lose energy and eventually detach from the top of the cylinders, resulting in the formation of small eddies that moved in the same direction during co-rotation.

Furthermore, when the rotational speed approached the critical value and exceeded it, a more complex phenomenon emerged—forming a virtual body between the cylinders. This virtual body acted as a barrier, impeding fluid flow between the cylinders. As the fluid moved rapidly near the cylinders, it circulated around them due to the combined effects of rotational and linear velocities, creating the perception of a virtual body in the flow field.

The velocity streamlines at this state simulated potential flow around this virtual body, which, in appearance, resembled a snowman, particularly in the counter-rotation case. The formation of this virtual body had a significant impact on the flow dynamics, particularly in suppressing the eddies that would otherwise wrap around the cylinders due to the fluid's rotational motion. This suppression of eddies was primarily due to the obstruction created by the virtual body, which altered the flow field and reduced the intensity of vortex formation around the cylinders.

This observation highlights the complex interplay between rotational speed, pressure gradients, and fluid dynamics in-cylinder flows, demonstrating how critical speeds and rotational directions can lead to vastly different flow patterns and physical phenomena. The presented findings can be further supported by similar works and findings by Chan et al. 2021. Specifically, the researchers described both the observed dynamics and the phenomenon of stabilization at the presumed critical rotational speed. The described physics were validated by other, related studies. Liu et al. 2018 described the vortex dynamics and drag reduction of the counter-rotating cylinder arrangement. Smith and Jones presented the effects of the gap ratio and the angular speed on the two cylinders' wakes Smith & Jones, 2019. All these studies would, therefore, help understand the fluid dynamics in each of the cylinders surrounded by a co-rotation of their neighbors presented in the study.

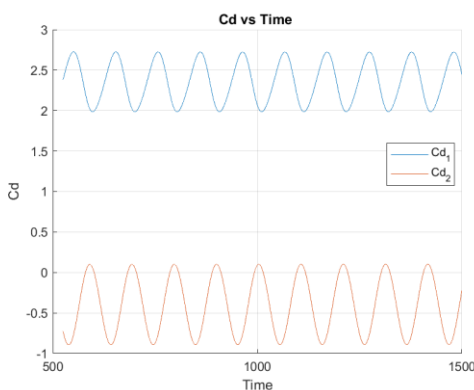


Figure 0-1 Time histories $\alpha = 3.0$ $g^* = 0.5$
 $Re = 50$

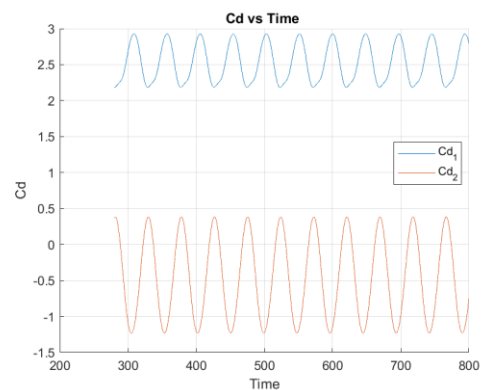


Figure 0-2 Time histories $\alpha = 3.0$ $g^* = 0.5$
 $Re = 100$

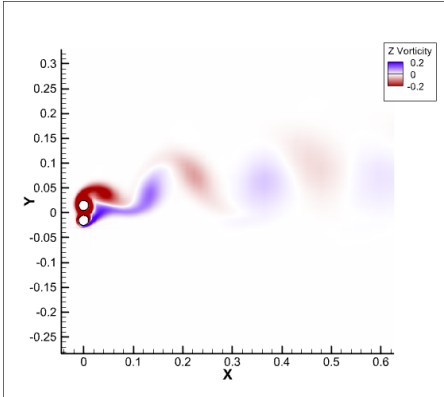


Figure 0-3 vorticity plot at $\alpha = 3.0 g^* = 0.5 Re = 50$

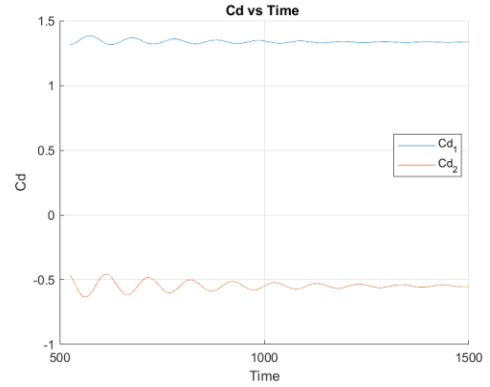


Figure 0-5 Time histories $\alpha = 3.5 g^* = 0.5 Re = 50$

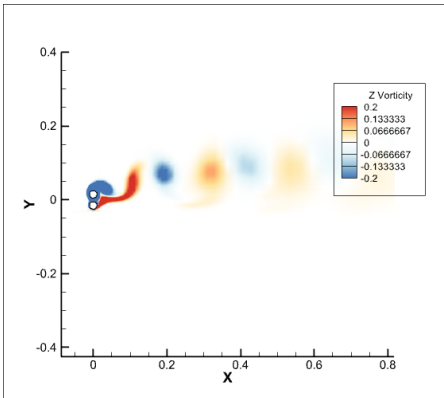


Figure 0-4 Vorticity plot at $\alpha = 3.0 g^* = 0.5 Re = 100$

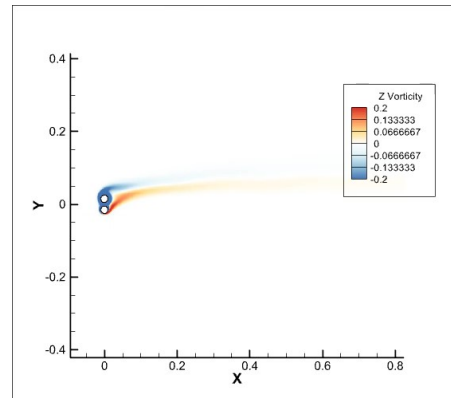


Figure 0-6 vorticity plots at $\alpha = 3.5 g^* = 0.5 Re = 50$

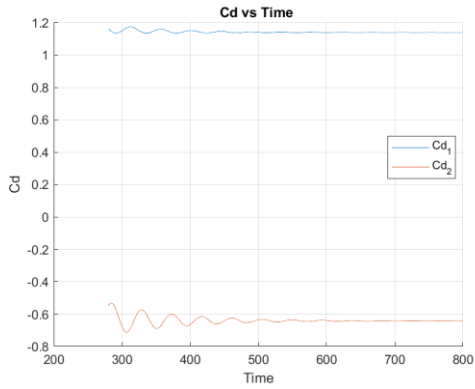


Figure 0-7 Time histories $\alpha = 3.5$ $g^* = 0.5$
 $Re = 100$

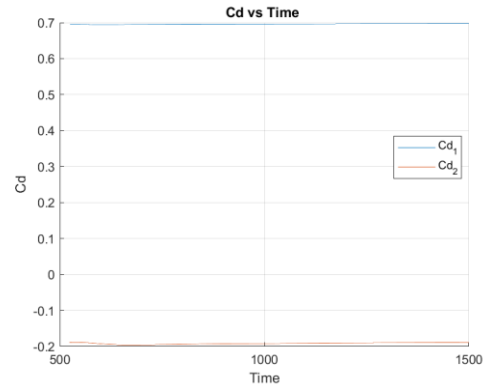


Figure 0-9 Time histories $\alpha = 4.0$ $g^* = 0.5$
 $Re = 50$

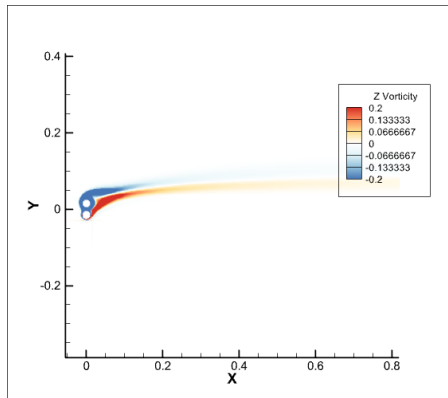


Figure 0-8 vorticity Plot at $\alpha = 3.5$ $g^* = 0.5$
 $Re = 100$

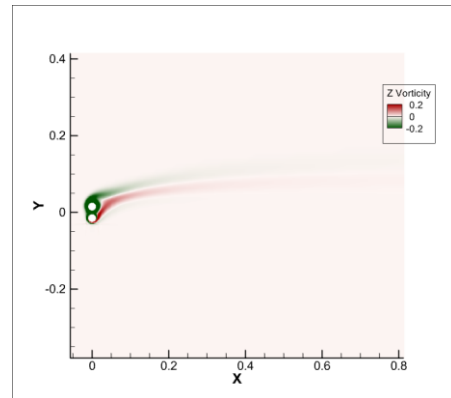


Figure 0-10 vorticity plot at $\alpha = 4.0$ $g^* = 0.5$
 $Re = 50$

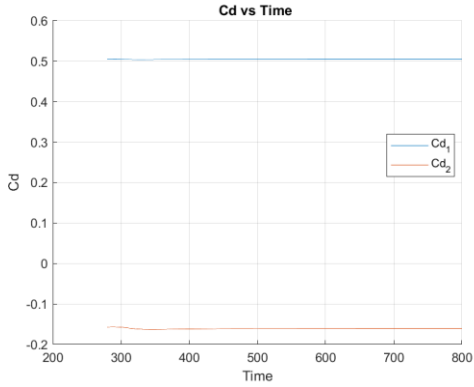


Figure 0-11 Time histories $\alpha = 4.0$ $g^* = 0.5$ $Re = 100$

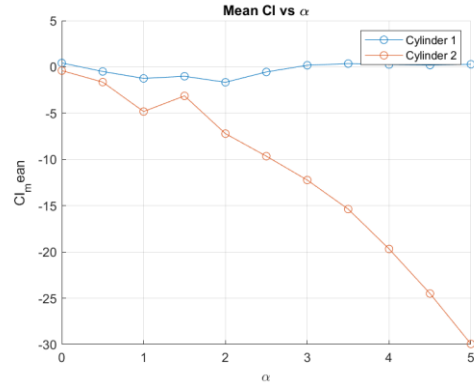


Figure 0-14 Mean Cl $g^* = 0.5$ $Re = 100$

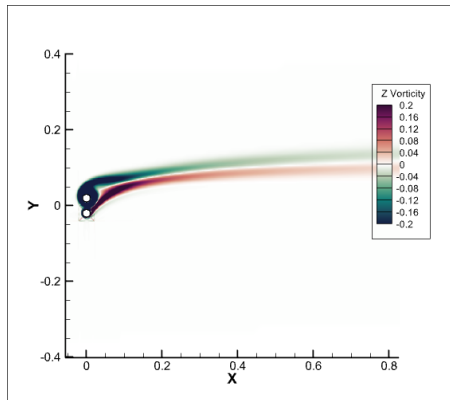


Figure 0-12 Vorticity plots at $\alpha = 4.0$ $g^* = 0.5$ $Re = 100$

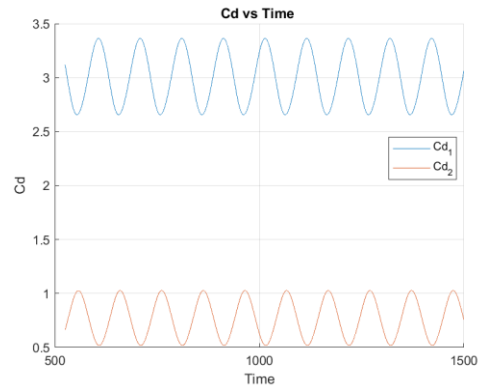


Figure 0-15 $\alpha = 1.5$ $g^* = 0.5$ Stable at $Re = 50$

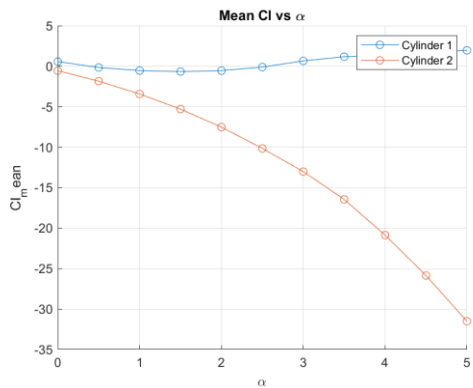


Figure 0-13 Mean Cl $g^* = 0.5$ $Re = 50$

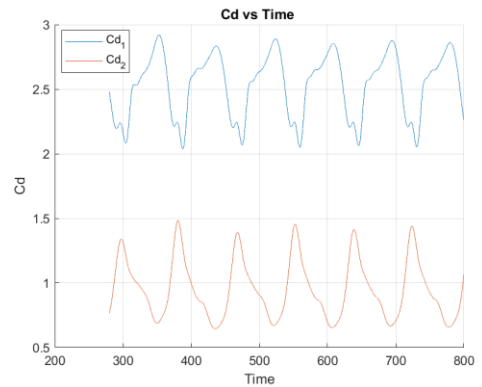


Figure 0-16 $\alpha = 1.5$ $g^* = 0.5$ Unstable at $Re = 100$

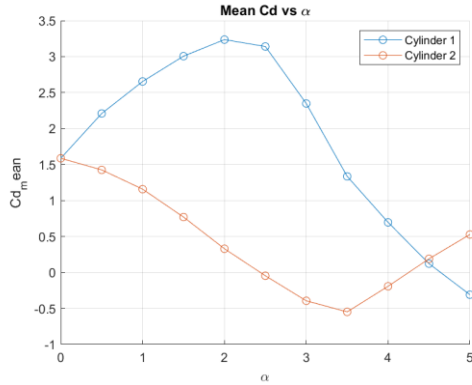


Figure 0-17 Mean drag $g^* = 0.5$ $Re = 50$

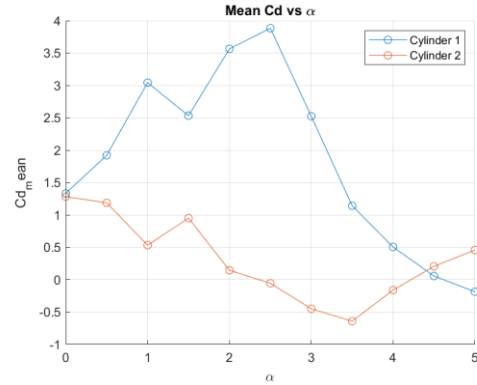


Figure 0-18 Mean drag $g^* = 0.5$ $Re = 100$ (right)

3.5.2 Gap spacing of 1 ($g^* = 1$)

By conducting the study on the phenomenon quantitatively, it is evident that the lift and drag characteristics of two vertically aligned, same direction rotating cylinders exhibit several types of behavior with the rotation speed due to several phenomena. These two types of phenomena are widely known and well over search on; however, some peculiar things were found while referring to Mittal & Kumar : 1. The simulation results on a Reynolds number are 50 showed that the anti-phase drag coefficient of both the upper and lower cylinder is clearly stable. The drag coefficient and the amplitude of vortex shedding increase until $\alpha = 2.5$ for the first cylinder dramatically, which is consistent with the observation of potential flow theory for the lift curve of a single rotating cylinder at $Re = 200$; $0 < \alpha < 5$. The drag coefficient continuously further decreased exponentially; 2. Both in lift coefficient observations, the coefficient continuously decreased until 2.5, and then the decrease is not long observed. It is noteworthy that the average lift coefficient of the lower cylinder decreased with higher speed until it reached 3.5, after which it began to increase back. This can lead C_d to lower value due to falling below the x-axis, meaning that it yields the thrust force. This finding indicates that it is not uncommon for dragging force not only to be counteracted but transformed into pushing force.

At $Re=100$, the flow regimes for different values of α transited through multiple stages with rotation speed. Asynchronous vortex shedding was highly unstable at $0 < \alpha < 1$ up to

which is shifted to an anti-phase single frequency mode at $\alpha=1$ resulting in still unstable asymmetric vortex shedding. The flow continued in the anti-phase single frequency mode until $\alpha=3$ and it becomes stable for $\alpha=3.5$ until

$\alpha=4$. The transitions of flow regimes are important to understand the dynamics of a vortex and its suppression by rotating. Moreover, the transition values for several modes help understand the fluid dynamics of flow. Both the drag coefficient 'C' and the frequency components followed the same trend there is an exponential increase until $\alpha=2.5$ peaking, after which it due to the same trend. The mean lift 'C' of the bottom cylinder is observed to decrease with rotation up to $\alpha=5$ values. However, beyond $\alpha=3.5$, its increases which indicate the changes in fluctuations. The results of rotation flow on two same-direction cylinders can be compared to counter-rotation of cylinders in which the lift and drag coefficients behaved differently. As in most counter-rotating cylinder results, the critical rotation plays a vital role in the behavior of lift and drag coefficients. In this case of rotating in the same direction, the modes were different due to the nature of the stable critical speed ' α_{crit} '. The mean lift coefficient of the lower cylinder decreased until a rotational speed at 5 of α , which is indicative of a strong dependency on rotational dynamics. The decrease suggests that the impact of the interaction of the two cylinders is great on the overall lift force. The negative drag coefficient values observed that denote thrust are of particular interest since they imply promising features in the thrust generation system. A virtual body was created from the critical rotational speed and above towards the surface of the cylinders. No fluid is left between the cylinders, since the fluid circulates at high speeds near the rotating cylinders. Although counterclockwise fluid continues, it moves with the rotational velocity of the fluid, and the fluid column tends to circulate around the cylinders. It is as if the fluid perceives a virtual body created where the velocity streamlines are as seen in a potential flow outside the virtual object. In the case of counter-rotation, the virtual body features an ellipse, whereas in terms of co-rotation, it features a snowman shape. At angular speeds lower than the critical rotational speed, there is still residual flow of fluid between the cylinders. As depicted in fig. 10, one can see the looseness of the area below and above the cylinder, where the pairs of vortices are created. Two pairs of the fluid ingested are created by both cylinders; some are counterclockwise, others are clockwise.

The flow is blocked by the rotating an ingested fluid, and by the centrifugal forces, there gets wrapped around the cylinder and phenotyping force. This implies that the vortices are generally suppressed. Hence, these assumptions suggest that the findings align with Chan et al. 2011, which created the identical vortex suppression analysis in a counterclockwise angle.

This study has practical relevance to a variety of engineering and industrial disciplines. The performance of fluidic machinery can be optimized by properly selecting cylinder rotational speeds and gap ratios. This could reduce energy usage and boost vehicle or structure aerodynamics if applied to vehicles and various facilities..

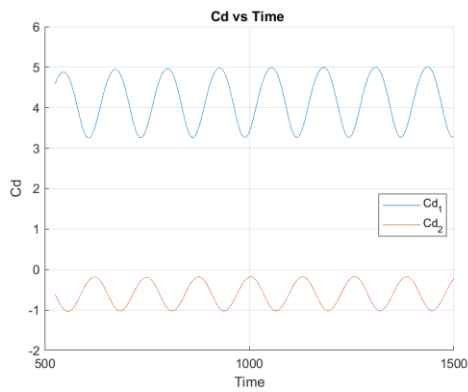


Figure 0-19 Time histories $\alpha=3.0$ $g^*=1$ at $R = 50$

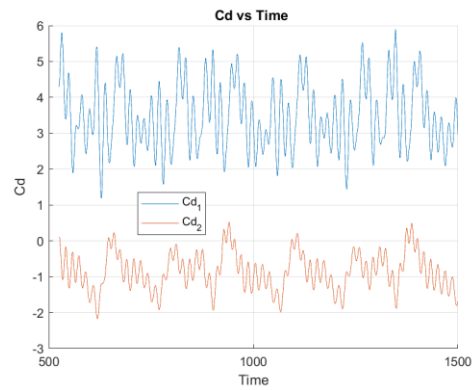


Figure 0-21 Time histories $\alpha = 3.0$ $g^* = 1$ at $Re = 100$

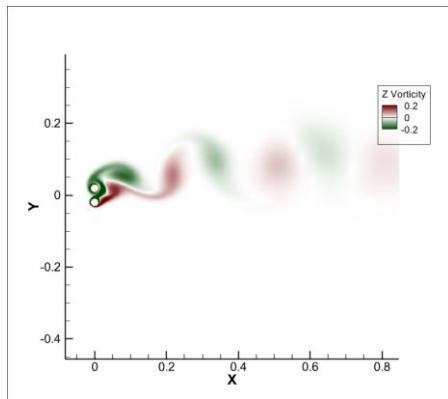


Figure 0-20 Vorticity at $\alpha = 3.0$ $g^* = 1$ $Re = 50$

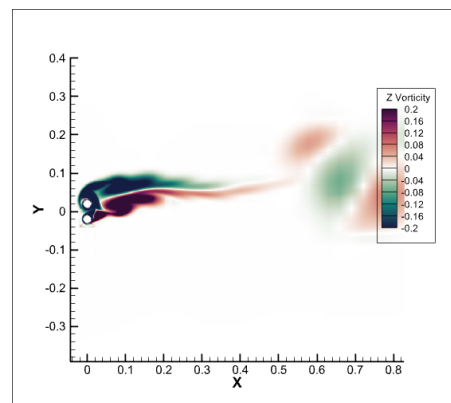


Figure 0-22 vorticity plot at $\alpha=3.0$ $g^*=1$ $Re = 100$

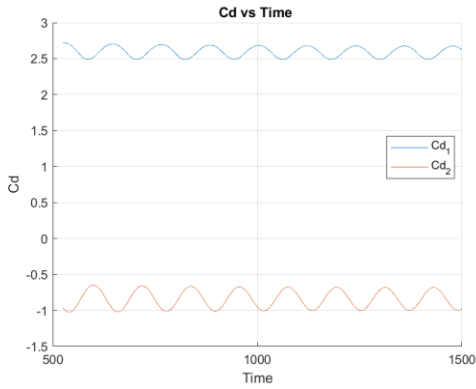


Figure 0-23 Time histories $\alpha = 3.5 g^* = 1$ stable at $Re = 50$

Figure 0-25 Time histories $\alpha = 3.5 g^* = 1$ stable at $Re = 100$

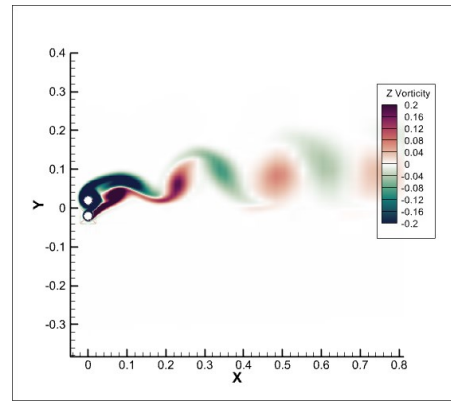


Figure 0-26 Vorticity plots at $\alpha = 3.5 g^* = 1$ stable at $Re = 100$

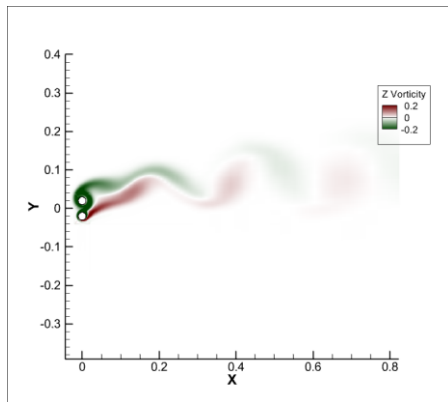


Figure 0-24 Vorticity plots at $\alpha = 3.5 g^* = 1$ $Re = 50$

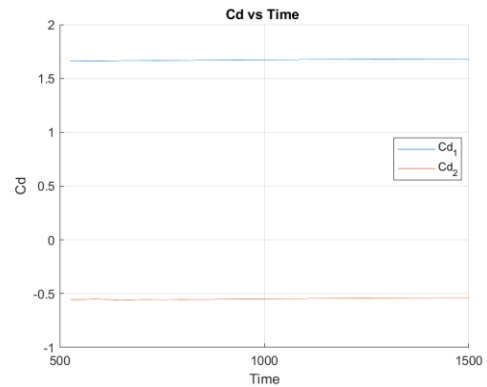
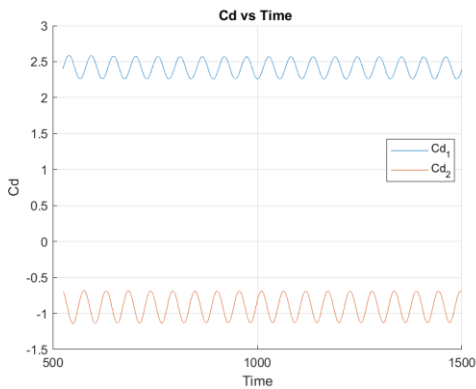


Figure 0-27 Time histories $\alpha = 4.0 g^* = 1$ $Re = 50$



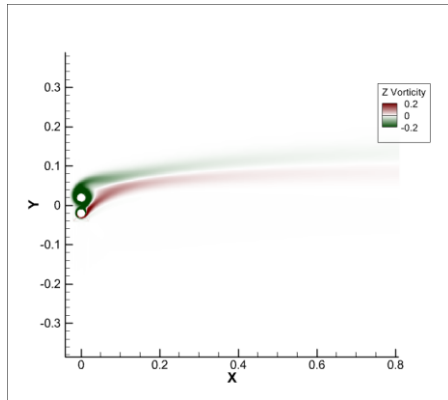


Figure 0-28 Vorticity plots at $\alpha = 4.0$ $g^* = 1$ stable at $Re = 50$

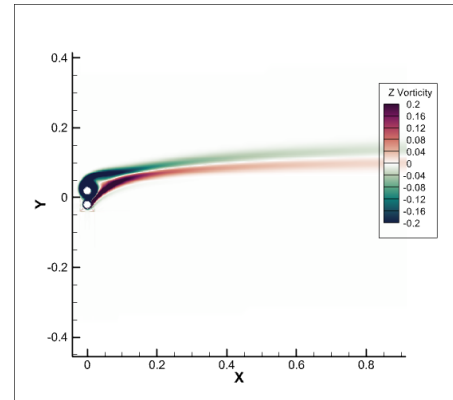


Figure 0-30 Vorticity plots at $\alpha = 4.0$ $g^* = 1$ stable at $Re = 100$

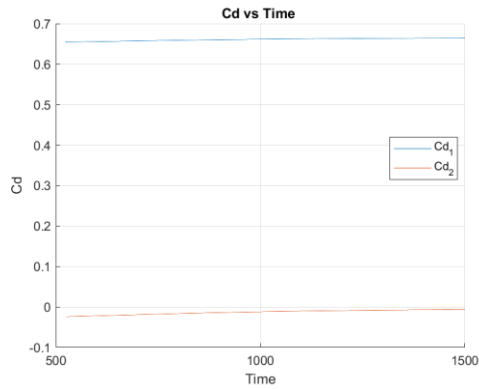


Figure 0-29 Time histories $\alpha = 4.0$ $g^* = 1$ $Re = 100$

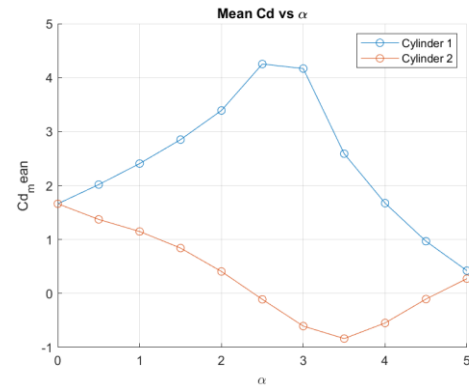


Figure 0-31 Mean Cd $g^* = 1$ $Re = 50$

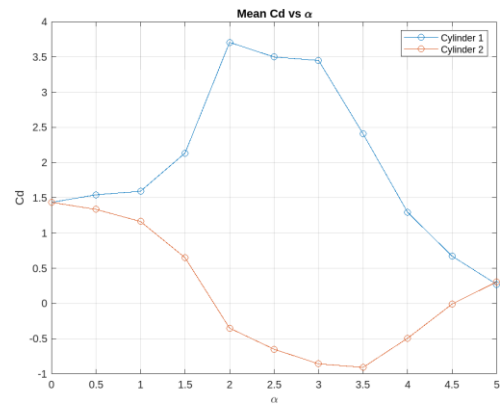


Figure 0-32 Mean Cd $g^* = 1$ $Re = 100$

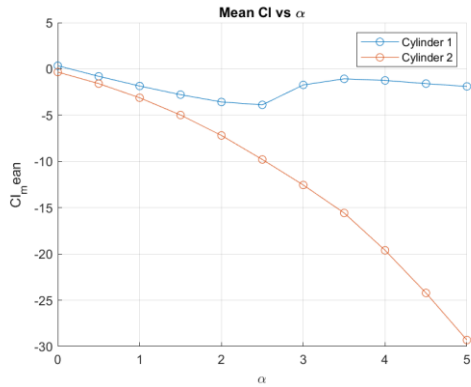


Figure 0-33 Mean Cl $g^* = 1.0$ $Re = 50$

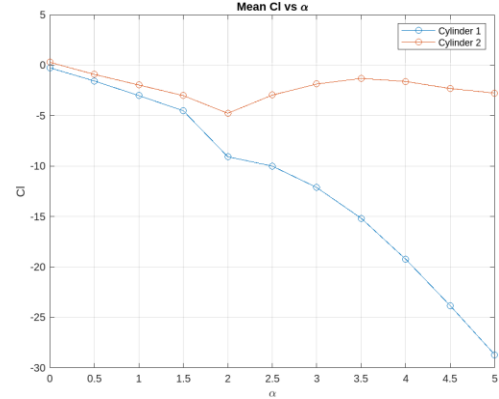


Figure 0-34 Mean Cl $g^* = 1.0$ $Re = 100$

3.5.3 Gap Ratio of 3.0 ($g^* = 3.0$)

From the results of our investigation, it is seen that the behavior of the rotating cylinders under different gap ratios and rotational rates presented crucial information in the highlights of the vortex dynamics, reduction in drag, and the lift coefficient. Our research matched the findings of Chen et al. , which expanded particularly by Chen et al. on the measures which affect the suppression of vortex and the reduction of drag in terms of the counter-rotating of the two cylinders. On our observations under the unsteady counter-rotating conditions, the cylinders could be seen to rotate at high velocities to simulate the outcomes of the virtual elliptical body when the value of gap ration, the cylinder diameter, and spacing ration, was set to 3. This was previously the rotating condition reduced to a steady bend according to the observations done by Chen et al. whereas our observations on a fluid flowing rotating condition were described provided to a steady bend on vortex suppression. The vortices from the rotating lower cylinder were absorbed into the upper cylinder's rotational wake, suppressing the single vortices. This had demonstrated a complex interaction with the vortices surrounding the rotational cylinder wake. At Reynolds number, Re , of 50, the results indicated that the secondary region of instabilities which were progressively seen at maximum rotational were able to reappear. Initially, the vortices were suppressed by the rotational radius, but at maximum rotation, the vortices re-established during which this indicated a clear correlation to the rotational dynamics. This had meant that the critical rotation velocity was almost equal to that of a single cylinder.

The effect of the Reynolds number on the drag coefficient was also instructive. At $Re=100$, for both cylinders, the in-phase vortex shedding phenomenon was consistent. As the two cylinders' rotation rate increased, the amount of drag experienced by the cylinders' mean decreased, hitting the valley for both cylinders when the rotation rate was $\alpha=3.5$. This would generally mean that there is a certain rate of rotation at which the drag is minimized. Conversely the drag started increasing again after the valley, and this may have been as a result of the re-establishment of the vortices at the centroid, which was less frequent and high amplitude. The debut suppression at $\alpha=2$ and reappearance at $\alpha=4$, only to die down again at $\alpha=5$, is a major indicator of the dynamics of vortex behavior in relation to the two cylinders' rotation. These results were in agreement with what was observed by Chan et al; irrespective of the rotation condition, the vortices re-established once more suppression. For $Re=50$, a consistently anti-phase drag coefficient was noted. As the rate of rotation of the cylinders increased, the average drag for the two cylinders decreased, hitting the valley for the two cylinders when the cylinder was rotating at $\alpha=3.5$. Past the valley, the mean drag indicated a gradual ascent. It can thus be inferred that there is much influence of the revolving speed at low Re values of the rotational dynamics, which is relevant in assessing the best drag suppression technique.

Finally, the lift coefficient response to changing rotation rates also indicates the highly complicated fluid dynamics approaches. The mean lift coefficient decreased as the rotation of the cylinder increased. But the lift coefficient behaved in-phase, and as the rotation remained in-phase, the amplitude of the lift coefficient increased with the increase in rotation, but the amplitude of the secondary instability was higher than that of the primary instability. It, therefore, indicates that secondary mechanisms play a more critical role in acting lift forces at the high rotation. As the mean of lift decreased, and the amplitude increases, indicates that there is a direct relationship between rotation and lift force mechanisms. The relative higher amplitude of the secondary makes it more functional in acting lift forces at high rotations. This study provides relevant information on vortex suppression and drag reduction of a rotating cylinder, supporting and contributing to Chan et al. investigations. The study focuses on the effect of rotation rate and gap width in the reduction of drag and importance of each in the dynamics behavior of the interaction between current and subsequent cylinder. Through our study, it is possible to conclude that

the lift forces affect the cylinder and drag reduce which is feasible at the counter-rotating condition it was not evaluated in other studies.

The findings of this study have immediate, but still far-reaching, implications for a range of engineering and industrial disciplines. Adjusting the rotation speeds and spacing proportions between cylinders can improve the functionality of fluid machinery, lower energy consumption, and make vehicles and structures more aerodynamically effective.

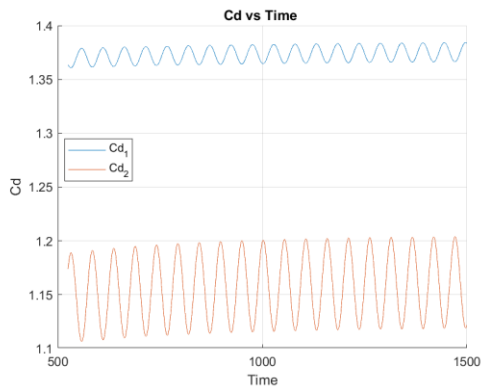


Figure 0-35 Time histories $\alpha = 1.5 g^* = 3$ stable at $Re = 50$

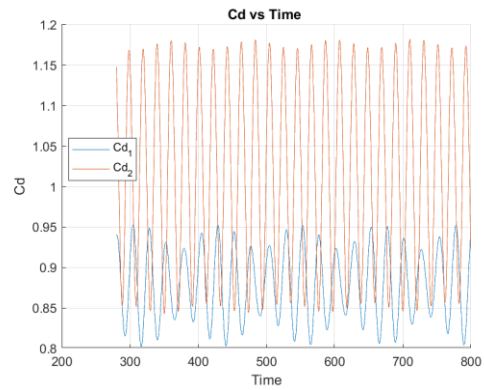


Figure 0-37 Time histories $\alpha = 1.5 g^* = 3$ unstable at $Re = 100$

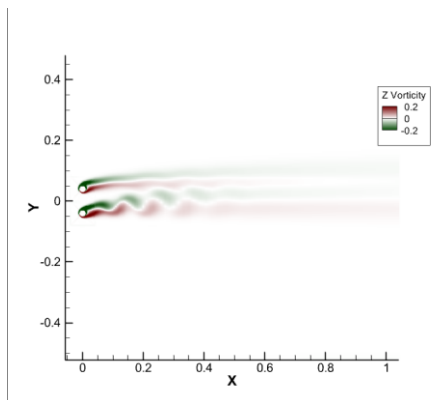


Figure 0-36 Vorticity plots at $\alpha = 1.5 g^* = 3$ stable at $Re = 50$

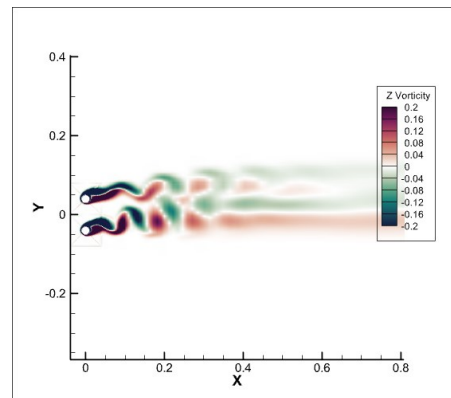


Figure 0-38 Vorticity plots at $\alpha = 1.5 g^* = 3$ $Re = 100$

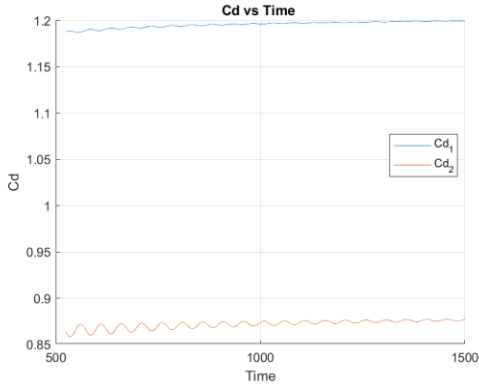


Figure 0-39 Time histories $\alpha = 2.0$ $g^* = 3$ stable at $Re = 50$

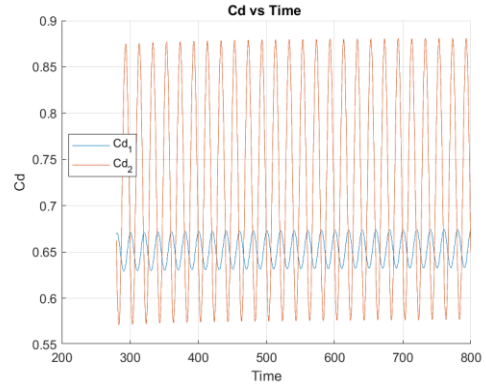


Figure 0-41 Time histories $\alpha = 2.0$ $g^* = 3$ unstable at $Re = 100$.

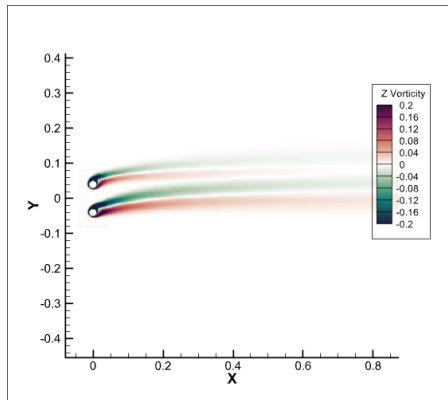


Figure 0-40 Vorticity plot at $\alpha = 2.0$ $g^* = 3$ at $Re = 50$

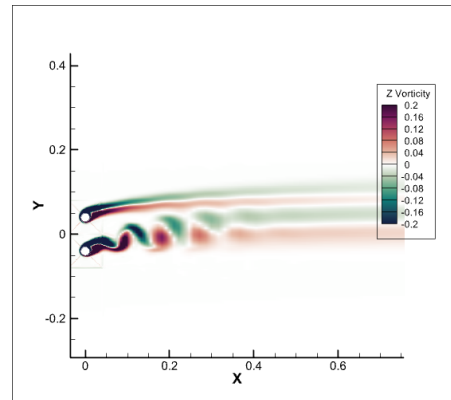


Figure 0-42 Vorticity plot at $\alpha = 2.0$ $g^* = 3$ at $Re = 100$

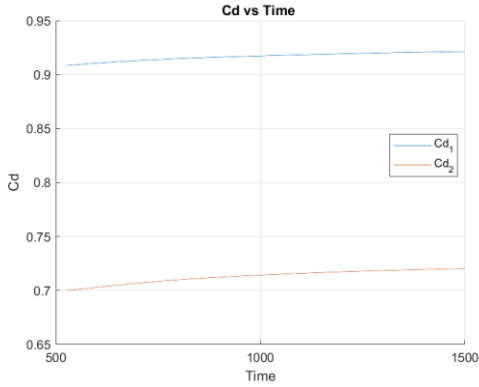


Figure 0-43 Time histories $\alpha = 2.5$ $g^* = 3$ stable at $Re = 50$

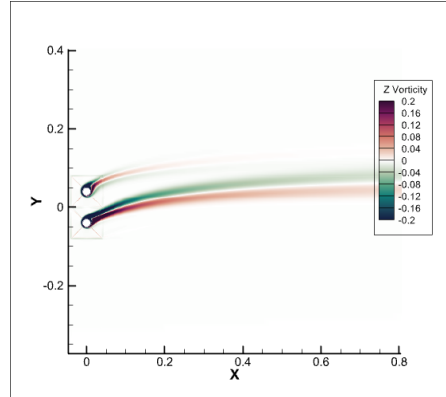


Figure 0-46 Vorticity plot at $\alpha = 2.5$ $g^* = 3$ $Re = 100$

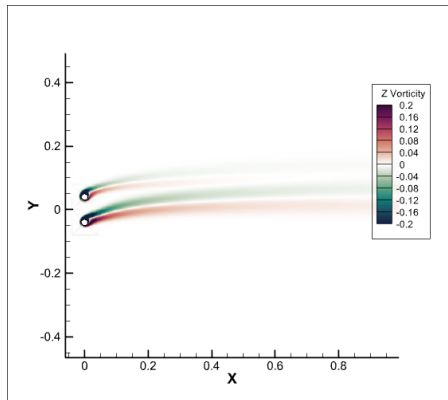


Figure 0-44 $\alpha = 2.5$ $g^* = 3$ $Re = 50$

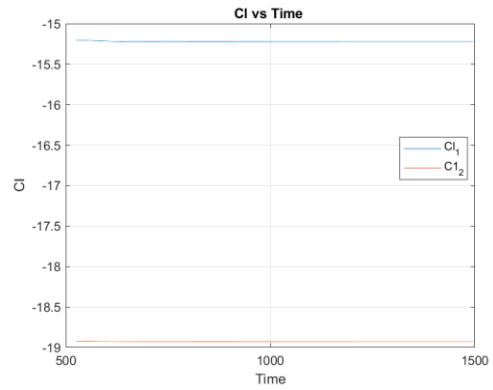


Figure 0-47 Time histories $\alpha = 4.0$ $g^* = 3$ stable at $Re = 50$

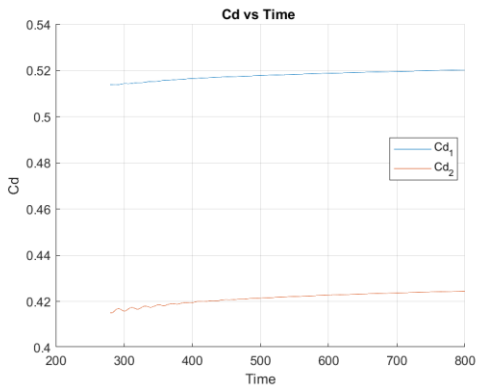


Figure 0-45 Time histories $\alpha = 2.5$ $g^* = 3$ at $Re = 100$

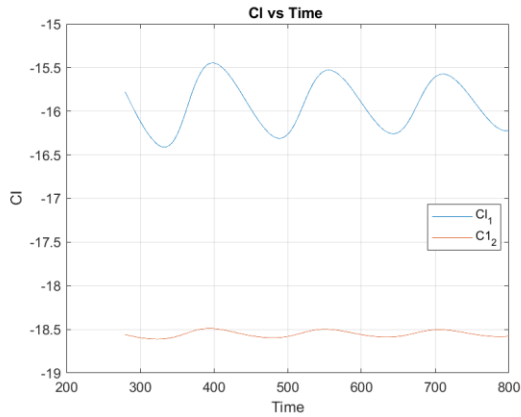


Figure 0-48 Time history $\alpha=4$ $g^* = 3$ at $Re = 100$

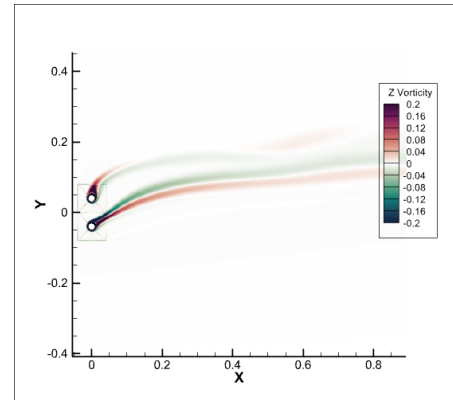


Figure 0-49 Secondary instability at $\alpha = 4.0$ $g^* = 3$ at $Re = 100$

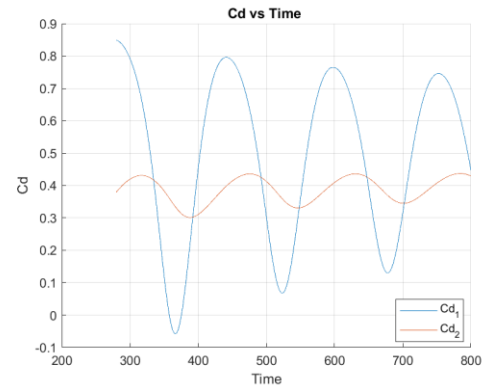


Figure 0-50 Time history $a= 4$ $g^* = 3$ at $Re = 100$

3.5.4 Dynamic Mode Decomposition

Flow Regimes and Vortex Dynamics

In this study, we have investigated the complex flow regimes and vortex dynamics of two side-by-side rotating cylinders at varying non-dimensional rotational speeds α and gap spacings (g^*). The flow physics, characterized by the evolution of vortex structures and their interactions, provides crucial insights into the transition of flow regimes as the rotational speed increases.

Case 1: $g^*=0.5$, $Re = 100$, $\alpha = 1$

At a gap spacing of $g^*=0.5$ and a rotational speed of $\alpha=1$, the flow regime is dominated by in-phase vortex shedding. The DMD analysis shows that the vortices shed from both cylinders are synchronized, leading to a stable and symmetric wake pattern. The interaction between the wakes is relatively weak due to the low rotational speed, resulting in a smooth and orderly flow. This configuration represents the initial stage where the flow remains laminar with minimal perturbations.

Case 2: $g^*=0.5$, $Re = 100$, $\alpha=1.5$

As the rotational speed increases to $\alpha=1.5$, the flow begins to transition into a more complex regime. The in-phase vortex shedding observed at $\alpha=1$ starts to destabilize, giving rise to secondary vortex structures. The DMD results indicate the emergence of higher frequency modes, suggesting the onset of an anti-phase shedding regime. The interaction between the wakes becomes more pronounced, leading to increased flow instability and the potential for vortex pairing or merging. This stage marks the beginning of a transition from a laminar to a more turbulent flow regime.

Case 3: $g^*=1$, $Re = 100$, $\alpha=1.5$

Increasing the gap spacing to $g^*=1$ while maintaining $\alpha=1.5$ introduces further complexity into the flow dynamics. The flow regime remains in the anti-phase shedding mode, but with more pronounced vortex interactions. The larger gap allows for more independent vortex formation from each cylinder, reducing direct wake interactions while increasing the overall turbulence. The flow at this stage is characterized by a mix of coherent structures and chaotic fluctuations, indicative of a transitional flow regime moving towards turbulence.

Case 4: $g^*=1$, $Re = 100$, $\alpha=2$

At $\alpha=2$, the flow regime enters a highly unstable and turbulent state. The DMD analysis reveals a dominance of secondary and tertiary modes, indicating the breakdown of coherent vortex structures. The increased rotational speed enhances the centrifugal forces, further

destabilizing the flow and leading to the formation of irregular vortex patterns. The flow is now fully turbulent, with little to no coherence in the wake structures, and the interaction between the wakes of the cylinders becomes increasingly chaotic.

Case 5: $g^*=1$, $Re = 100$, $\alpha=3$

Finally, at the highest rotational speed of $\alpha=3$, the flow regime is fully developed turbulence. The DMD results show a broad spectrum of high-frequency modes, with energy distributed across multiple harmonics. The vortex shedding is highly irregular, with frequent vortex breakdowns and reformation. The chaotic nature of the flow at this stage is characterized by rapid changes in the velocity field and pressure distribution, leading to significant fluctuations in the aerodynamic forces acting on the cylinders.

Interpretation and Flow Physics

The transition of flow regimes with increasing rotational speed can be explained through the interplay of shear layer, pressure gradients, and vortex dynamics. At lower rotational speeds, the shear layers are relatively weak, allowing for synchronized vortex shedding and stable wake patterns. As the rotational speed increases, these shear forces become more significant, disrupting the flow and forming secondary vortices and the transition to anti-phase shedding. Beyond a critical speed, the flow becomes fully turbulent, characterized by irregular and chaotic vortex structures.

The observed flow regimes are consistent with the known vortex shedding behavior in rotating cylinder systems. As noted in previous studies, the critical rotational speed α_{crit} plays a crucial role in determining the stability of the flow. At speeds below α_{crit} , the flow remains stable, while speeds above this threshold lead to turbulence and the breakdown of coherent structures.

CONCLUSION

In sum, this study offers a rigorous analysis of varying gap ratios and Reynolds numbers of co-rotating side-by-side cylinders to identify the vortex suppression characteristics, drag reduction, and lift coefficient behaviors. The results provide unique insights into the rotational speed and gap spacing's impact on fluid flow tendency and wake stabilization through the cylinders' vortex street. These findings have critical implications across various applications of engineering, offering opportunities for major improvements in the fluid flow management and control of the cased rotating objects. For instance, an interesting observation on the role of the gap ratio was made, especially on the interactions of the vortex streets of the cylinders. As the gap spacing between the cylinders increased, their vortex street interactions reduced, requiring higher critical rotational speeds to achieve relatively the same wake instability suppression. However, relatively low rotational speeds critical coefficients greater than 3.5 remained effective across all considered cases. This observation is critical in applications that require a balance between space allowance and fluid flow stability, such as turbine blade and heat exchanger tube designs.

One of the main findings of our study was the effect of the Reynolds number on co-rotating cylinders. Specifically, at a Reynolds number of 50, we observed stable anti-phase drag coefficients and in-phase lift forces for rotational speeds below the critical speed; thus, $\alpha_{crit} = 3.5$. Both drag and lift experienced a change in behavior patterns, as the drag coefficient of the lower cylinder changed to negative after the critical speed, suggesting thrusting. Similarly, with the Reynolds number set to 100, the viscous vortex street stabilized after $\alpha_{crit} = 3.5$ due to the absence of secondary instability up to $\alpha = 5$. However, as the Reynolds number rose, the unstable vortex shedding model caused high variations in drag and lift coefficients. Our observations confirm the intricate relationship between fluid dynamics and rotational speed. The above discussion regarding the co-rotating vortices is consistent with the findings observed by Chan et al. in 2021 and offers more insight on the vortex suppression or destabilizing features.

Finally, the lift and drag properties of the cylinders at varying Reynolds numbers and rotating rates add more depth to the complexity surrounding the associated fluid mechanics. Different lift and drag coefficient changes were observed relative to the Reynolds number and rotation rate. The lower cylinder has the mean lift coefficient decreasing down to $\alpha = 5$, suggesting strong rotational dynamics effects. On the other hand, drag coefficients were observed to be negative, implying thrusts, which can be useful in certain applications such as propulsion systems. Prospective applications in propulsion include rotating the cylinders at optimally high rotating rates for the efficient utilization of the spontaneous flow energy given that it has been already determined. This indicates that the insight may be applied in fuel-efficient propulsion systems in aerospace and marine engineering fields where induced thrust isn't costly. Ultimately, the current research has numerous practical implications related to a broader range of engineering fields. The speed of the rotating cylinders, optimal gap ratios, and other relevant parameters could be used to improve the performance of fluid power units, reduce energy consumption, and optimize aerodynamics when designing various structures and vehicles. For example, the aerospace industry could use the insights from this research to enhance the design of wings using optimized vortex-harnessing techniques to reduce fuel consumption. Additionally, similar results could be used in automobile engineering. It is possible to reduce the cost of producing drag pressure through drag-reduction methods to boost the performance of vehicles and minimize harmful CO₂ emissions. In the marine engineering sector, the flow around rotating objects could enhance the performance of propulsion systems and control the movement of large vessels more efficiently. Thus, all these and many other applications demonstrate the significance of the current research.

To sum up, the gap ratio, rotational speed, and Reynolds number have a great influence on the dynamics of co-rotating side-by-side cylinders. According to the results of the research, gap spacing has an inverse relationship with the intensity of interaction between the vortex streets, which requires higher critical rotational speed in order to suppress the wake instability. The formation of a virtual body at its critical speed and its effect on the fluid flow are crucial for the practical implementation of engineering solutions. Due to these results, it is also possible to notice that there is a different pattern of the behavior for the lift and drag coefficients for the different Reynolds numbers. Such

the performance pattern is a manifestation of the complex reliance of the fluid dynamics on the rotational speed explained in this research. These findings can offer the guidance for the maximization on the efficiency of performance for fluid machinery and various aerodynamic systems in the fields of engineering. Based on the understanding of the vortex dynamics and its management mechanisms, such work can contribute to more feasible ways of the fluid control.

REFERENCES

- [1] Williamson, C. H. K. 1985 Evolution of a single wake behind a pair of bluff bodies. *J. Fluid Mech* vol 159, 1–18
- [2] Xu, S. J., Zhou, Y. & So, R. M. C. 2003 Reynolds numbers affect the flow structure behind two side-by-side cylinders. *Physics of. Fluids*, Vol 15, 1214
- [3] Kim, H. J. & Durbin, P. A. 1988 Investigation of the flow between a pair of circular cylinders in the flopping regime. *J. Fluid Mech*, Vol 196, 431–448.
- [4] Sumner, D., Wong, S. S. T., Price, S. J. & Paidoussis, M. P. 1999 Fluid behavior of side-by-side circular cylinders in steady crossflow. *J. Fluids Struct*, Vol 13, 309–338
- [5] Yoon, H. S., Kim, J. H., Chun, H. H. & Choi, H. J. 2007 Laminar flow past two rotating cylinders in a side-by-side arrangement. *Phys. Fluids*, Vol 19, 128103-1-128103-4
- [6] Chan, A. S. & Jameson, A. 2010 Suppression of the unsteady vortex wakes of a circular cylinder pair by a doublet-like counter-rotation. *Intl J. Num. Meth. Fluids*, Vol 63, 22–39.
- [7] Andre S. Chan & Peter A. Dewey 2011 Vortex suppression and drag reduction in the wake of counter-rotating cylinders. *J. Fluid Mech*, Vol 679, 343-382
- [8] Shaafi K, Naik S N and Vengadesan S 2017 Effect of rotating cylinder on the wake-wall interactions. *Ocean Engineering*, Vol 139: 275–286
- [9] Rana K, Manzoor S, Sheikh N A, Ali M and Ali H M 2017 Gust response of a rotating circular cylinder in the vortex suppression regime. *International Journal of Heat and Mass Transfer*, Vol 115, 763–776
- [10] Bayat R and Rahimi A B 2017 Numerical solution of threedimensional NS equations and energy in the case of unsteady stagnation-point flow on a rotating vertical cylinder. *International Journal of Thermal Sciences*, Vol 118, 386–396
- [11] Thakur P, Tiwari N and Chhabra R P. 2018 Power-law fluid flow across a rotating confined cylinder. *Journal of Non-Newtonian Fluid Mechanics* 251: 145–161

- [12] Strykowski BJ, Sreenivasan KR. On the formation and suppression of vortex ‘shedding’ at low Reynolds numbers. *J Fluid Mech* 1990, Vol 218, 71–107
- [13] Sakamoto H, Tan K, Haniu H. An optimum suppression of fluid forces by controlling a shear layer separated from a square prism. *J Fluids Eng* 1991, Vol 113, 183–9
- [14] Sakamoto H, Haniu H. Optimum suppression of fluid forces acting on a circular cylinder. *J Fluids Eng* 1994, Vol 116, 221–7.
- [15] Dalton C, Xu Y, Owen JC. The lift suppression on a circular cylinder due to vortex shedding at moderate Reynolds numbers. *J Fluids Struct* 2001 Vol 15, 617–28.
- [16] Agrawal, A., Djenidi, L. & Antonia, R. A. 2005 Investigation of flow around a pair of side-by-side square cylinders using the lattice Boltzmann method. *Comput. Fluids*, Vol 35, 1093–1107.
- [17] Abrahamsen Prsic, M., Ong, M. C., Pettersen, B. & Myrhaug, D. 2014 Large Eddy Simulations of flow around a smooth circular cylinder in a uniform current in the subcritical flow regime. *Ocean Eng.*, Vol 77, 61-73.
- [18] Karabelas, S. J. 2010 Large Eddy Simulation of high-Reynolds number flow past a rotating cylinder. *Int. J. Heat Fluid Flow*, Vol 31, 518-527.
- [19] Dol, S. S., Kopp, G. A. & Martinuzzi, R. J. 2008 The suppression of periodic vortex shedding from a rotating circular cylinder. *J. Wind Eng. Ind. Aerod.*, Vol 96, 1164-1184.
- [20] Lam, K. M. 2009 Vortex shedding flow behind a slowly rotating circular cylinder. *J. Fluid Struct.*, Vol 25, 245-262.
- [21] Ghazanfarian, J. & Nobari, M. R. H. 2009 A numerical study of convective heat transfer from a rotating cylinder with cross-flow oscillation. *Int. J. Heat Mass Tran.*, Vol 52, 5402-5411.
- [22] Paramane, S. B. & Sharma, A. 2010 Heat and fluid flow across a rotating cylinder dissipating uniform heat flux in 2D laminar flow regime. *Int. J. Heat Mass Tran.*, Vol 53, 4672-4683.

- [23] Rao, A., Thompson, M. C., Leweke, T. & Hourigan, K. 2015 Flow past a rotating cylinder translating at different gap heights along a wall. *J. Fluid Struct.*, Vol 57, 314-330.
- [24] Vakil, A. & Green, S. I. 2011 Two-dimensional side-by-side circular cylinders at moderate Reynolds numbers. *Comput. Fluid.*, Vol 51, 136-144.
- [25] Patankar, S. V. 1980 *Numerical Heat Transfer and Fluid Flow*. Taylor & Francis, New York.
- [26] Churchill, S. W. & Bernstein, M. 1977 A correlation equation for forced convection from gases and liquids to a circular cylinder in cross flow. *J. Heat Transfer, Trans. ASME*, Vol 94, 300-306.
- [27] Ramos-García, N., Sarlak, H., Andersen, S. J. & Sørensen, J. N. 2017 Simulation of the Flow Past a Circular Cylinder using an Unsteady Panel Method. *Comput. Fluid.*, Vol 147, 102-118.
- [28] Stringer, R. M., Zang, J. & Hillis, A. J. 2014 Unsteady RANS computations of flow around a circular cylinder for a wide range of Reynolds numbers. *Ocean Eng.*, Vol 87, 1-9.
- [29] Meneghini, J. R., Saltara, F., Siqueira, C. L. R. & Ferrari Jr., J. A. 2001 Numerical simulation of flow interference between two circular cylinders in tandem and side-by-side arrangements. *J. Fluid Struct.*, Vol 15, 327-350.
- [30] Chatterjee, D. & Sinha, C. 2016 Effect of Prandtl number and rotation on vortex shedding behind a circular cylinder subjected to cross buoyancy at subcritical Reynolds number. *Int. Commun. Heat Mass Tran.*, Vol 70, 1-8.
- [31] Thakur, P., Mittal, S., Tiwari, N. & Chhabra, R. P. 2016 The motion of a rotating circular cylinder in a stream of Bingham plastic fluid. *J. Nonnewton. Fluid Mech.*, Vol 235, 29-46.
- [32] Rao, A., Stewart, B. E., Thompson, M. C., Leweke, T. & Hourigan, K. 2011 Flows past rotating cylinders next to a wall. *J. Fluid Struct.*, Vol 27, 668-679.
- [33] Afroz, F., Sharif, M. A. R. & Lang, A. 2016 Numerical study of adverse pressure gradient generation over a flat plate using a rotating cylinder. *J. Fluid Struct.*, Vol 62, 187-208.

- [34] Kang, S. 2006 Uniform-shear flow over a circular cylinder at low Reynolds numbers. *J. Fluid Struct.*, Vol 22, 541-555.
- [35] Perret, L. 2009 PIV investigation of the shear layer vortices in the near wake of a circular cylinder. *Exp. Fluid*, Vol 47, 789-800.
- [36] Rajani, B. N., Kandasamy, A. & Majumdar, S. 2009 Numerical simulation of laminar flow past a circular cylinder. *Appl. Math. Model.*, Vol 33, 1228-1247.
- [37] Slaouti, A. & Stansby, P. K. 1992 Flow around two circular cylinders by the random-vortex method. *J. Fluid Struct.*, Vol 6, 641-670.
- [38] Alam, Md. M., Zheng, Q. & Hourigan, K. 2017 The wake and thrust by four side-by-side cylinders at a low Re. *J. Fluid Struct.*, Vol 70, 131-144.
- [39] Chen, W., Ji, C., Wang, R., Xu, D. & Campbell, J. 2015 Flow-induced vibrations of two side-by-side circular cylinders: asymmetric vibration, symmetry hysteresis, and near-wake patterns. *Ocean Eng.*, Vol 110, 244-257.
- [40] Elhimer, M., Harran, G., Hoarau, Y., Cazin, S., Marchal, M. & Braza, M. 2016 Coherent and turbulent processes in the bistable regime around a tandem of cylinders including reattached flow dynamics by means of high-speed PIV. *J. Fluid Struct.*, Vol 60, 62-79.
- [41] Gopalan, H. & Jaiman, R. 2015 Numerical study of the flow interference between tandem cylinders employing non-linear hybrid URANS – LES methods. *J. Wind Eng. Ind. Aerod.*, Vol 142, 111-129.
- [42] Kim, S. & Alam, Md. M. 2015 Characteristics and suppression of flow-induced vibrations of two side-by-side circular cylinders. *J. Fluid Struct.*, Vol 54, 629-642.
- [43] Liu, J., Xie, G. & Sundén, B. 2017 Flow pattern and heat transfer past two tandem arranged cylinders with oscillating inlet velocity. *Appl. Therm. Eng.*, Vol 120, 614-625.
- [44] Pang, J. H., Zong, Z., Zou, L. & Wang, Z. 2016 Numerical simulation of the flow around two side-by-side circular cylinders by IVCBC vortex method. *Ocean Eng.*, Vol 119, 86-100.
- [45] Thapa, J., Zhao, M., Cheng, L. & Zhou, T. 2015 Three-dimensional simulations of flow past two circular cylinders in side-by-side arrangements at right and oblique attacks. *J. Fluid Struct.*, Vol 55, 64-83.

- [46] Tu, J., Zhou, D., Bao, Y., Ma, J., Lu, J. & Han, Z. 2015 Flow-induced vibrations of two circular cylinders in tandem with shear flow at low Reynolds number. *J. Fluid Struct.*, Vol 59, 224-251.
- [47] Vakil, A. & Green, S. I. 2011 Two-dimensional side-by-side circular cylinders at moderate Reynolds numbers. *Comput. Fluid.*, Vol 51, 136-144.
- [48] Yeon, S. M., Yang, J. & Stern, F. 2016 Large-eddy simulation of the flow past a circular cylinder at sub- to super-critical Reynolds numbers. *Appl. Ocean Res.*, Vol 59, 663-675.